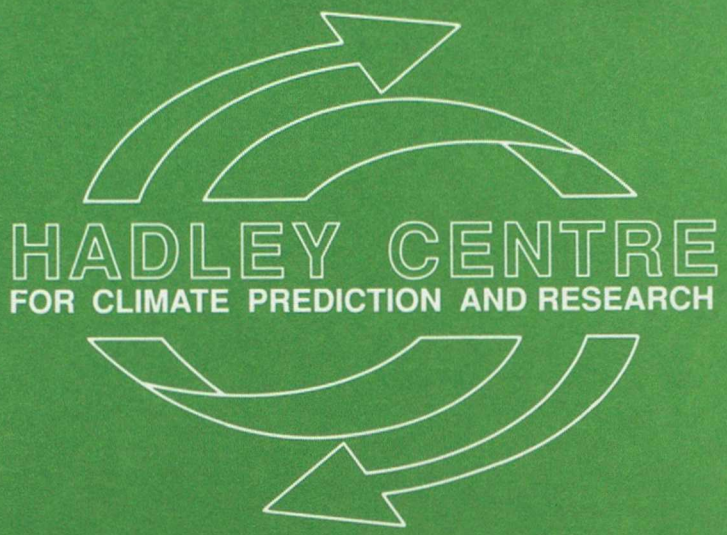

Deforestation of Amazonia - modelling the effects of albedo change.

by

M.F. Mylne and P.R.Rowntree

CRTN 7

January 1991

CLIMATE
RESEARCH
TECHNICAL
NOTE

Hadley Centre
Meteorological Office
London Road
Bracknell
Berkshire RG12 2SY

CLIMATE RESEARCH TECHNICAL NOTE NO. 7

DEFORESTATION OF AMAZONIA - MODELLING THE EFFECTS OF ALBEDO CHANGE

by

M F MYLNE AND P R ROWNTREE

Hadley Centre for Climate Prediction and Research
Meteorological Office
London Road
Bracknell
Berkshire RG12 2SY
U.K.

Abstract

The effects in climate models of changes in albedo and soil moisture which are expected to follow from deforestation of Amazonia are reviewed. Results from experiments with tropical forest regions (a) forested ("Experiment F") and (b) grass-covered ("Experiment G") are compared over South America. Then, Experiment F is compared with "Experiment 2" which has constant snowfree albedo of 0.2, close to that of grassland; in the South American region, the albedo changes for (G-F) and (2-F) are similar and, as Experiment 2 is an eight year run, assessments of the statistical significance can be made.

The results for December to February and March to May show a decrease of rainfall over Amazonia, and also to the southeast outside the area with changed albedos in (G-F). These decreases are common to both (G-F) and (2-F) and are statistically significant in the comparison with the eight year record for Experiment 2. In June to August, changes are small south of the equator because the rainbelt has moved north of the Amazon basin; larger, significant decreases are obtained north of the equator. The drying with increased albedo is due to decreases in both evaporation and moisture convergence. The decreases in evaporation result both from a reduction in absorbed energy at the surface and an increase in surface resistance to evaporation.

1. Introduction

Land clearance in areas of existing tropical rainforest results in removal of original forest and modification of agricultural practices. In addition to detrimental ecological impact (eg Poore, 1976) and enhanced erosion of fertile top soil (Salati and Vose, 1983), deforestation in the tropics could have an important influence on the local climate and may cause both regional and global climatic perturbations.

The sensitivity of 3D general circulation models (GCMs) to surface albedo has been reviewed by Henderson-Sellers and Wilson (1983), Mintz (1984) and Rowntree (1988). Charney et al. 1977, Chervin (1979), Sud and Fennessy (1982) and Planton (1986) have each performed experiments in which the surface albedo in a GCM was increased locally [relative to a control experiment]. All are for Northern Hemisphere summer. Although the magnitudes and locations of the albedo changes were different in each experiment the results were qualitatively similar (Table I).

The principal results (Table I) are:

(1) Evaporation was decreased in all cases

(2) Precipitation was decreased in all experiments except two where changes were small; both these were near mountain ranges (Rockies, Himalayas) and poleward of latitude 20°.

(3) Moisture convergence (P-E) was decreased in all but 3 cases, these 3 being poleward of latitude 20°.

Although, for Chervin's experiment, there is no direct evidence concerning (1) and (3), indirect evidence is provided by the maps showing decreased ascent and reduced soil moisture with increased albedo, especially over the Sahara.

For the areas equatorward of 20° latitude which are most relevant to this paper, the ratios of the fractional change in rainfall to the change in albedo (last column of Table I) average about -2 suggesting a 20% decrease in rainfall for a 0.1 increase in albedo. On average more than half the change is due to moisture convergence (P-E), though there is considerable variability in this, particularly between Charney et al's results and those of Sud and Fennessy. Carson and Sangster (1982) also found decreases in precipitation and evaporation and rises of surface pressure over most land points when a global scale increase in land surface albedo from 0.1 to 0.3 was introduced into the United Kingdom Meteorological Office (UKMO) 5 layer GCM.

Rowntree (1988) summarized two mechanisms by which albedo modification may affect the local climate. The reduction in net radiation (R_N) decreases the energy available for turbulent flux from the surface or downward transfer into the soil (G). For tropical conditions it was shown that the changes in latent heat flux will be a fraction $X = \frac{3}{4+r_s/r_{ae}}$ of the change in (R_N-G), where r_s and r_{ae} are the surface and atmospheric resistances to evaporation. X ranges from ~ 0.75 for a wet surface (r_s=0) to zero for a dry surface. For a moist surface with 250 Wm^{-2} average incident solar radiation it follows that an increase in albedo of 0.1 should reduce evaporation directly by 0.65 mm day^{-1}.

The second direct mechanism by which perturbation of the surface radiative properties can modify climate is that discussed by Charney (1975). Cooling of the local surface-atmosphere column due to an increase in surface albedo relative to adjacent regions can cause a decrease in ascent and associated rainfall. The consequent decrease in moisture convergence (P-E), shown in Table I, tends to reduce soil moisture. As soil moisture deficits increase, they begin to limit evapotranspiration, increasing the proportion of turbulent heat flux in sensible form.

Such changes in fluxes of moisture and heat may alter the stability of the atmospheric column and the relative humidity and precipitation in the region of perturbation. The responses of various GCMs to prescribed changes in moisture availability (β) are summarized in Table II. The moisture availability function, β, is used to scale the actual evaporation relative to its calculated potential value as a function of soil moisture content. In many sensitivity studies (for example Shukla and Mintz, 1982, Rowntree and Bolton 1983, Suarez and Arakawa (as reported in Mintz, 1984), Yeh et al, 1984 and Cunnington and Rowntree 1986) a reduction in moisture availability and consequently evaporation has been shown generally to result in reduction in precipitation. This helps to maintain the soil moisture deficits. The gain in direct heating of the atmosphere from increased sensible heat flux may be offset by a reduction in latent heat release if the precipitation is reduced. Note that the direct reduction in evaporation due to albedo, discussed earlier, similarly tends to reduce precipitation.

The experiments discussed above show that models are sensitive to the treatment of land surface processes. Comparatively few experiments have been designed specifically to test model sensitivity to aspects of tropical deforestation. Potter et al. (1975) considered the impact of increasing surface albedo in a portion of the tropical zone of the Lawrence Livermore 2D statistical dynamical model. Two perturbation experiments were performed. In the first (dry case) the albedo increase was combined with an imposed increase in runoff and restricted evaporation. In the second (wet case) only the change in albedo was prescribed. Decreases in global precipitation and temperature were obtained for the "wet case" deforestation. A slightly smaller decrease in temperature was found to occur in the "dry case" due to the associated reduction in evaporative cooling of the surface.

Henderson-Sellers and Gornitz (1984) replaced forest by grassland in the Amazon region in the Goddard Institute for Space Studies (GISS) GCM. In this experiment surface roughness length, the effective rooting depth, the moisture capacity of the two soil layers and surface albedo were all adjusted. A decrease in annual mean precipitation of about 0.6 mm day^{-1} resulted in Amazonia. The reductions in rainfall and moisture holding capacity caused a reduction in the mean moisture content of both soil layers. Evaporation from the surface decreased. A reduction in the predicted cloud amount increased the surface incident solar radiation. For surface temperature these two effects were found to offset partially the impact of the increase in surface albedo and overall little systematic change was found. The authors identified the need for further investigation with this and other GCMs to confirm that similar results can

be obtained with models containing different physics and with different control simulations. Any major physical response to surface perturbation should be replicable qualitatively in a model of similar complexity.

Towards this goal, Dickinson and Henderson-Sellers (1988) have simulated deforestation of the Amazon region using the Biosphere-Atmosphere Transfer Scheme in the NCAR Community Climate Model. Major changes imposed included decreases in the vegetation cover, aerodynamic roughness length, sensitivity of vegetation stomata to radiation, and total soil depth, and increases in the proportion of rainfall contributing to runoff (which is itself a function of vegetation cover), vegetation and soil albedos and density of vegetation roots in an upper soil layer. Evaporation for the most part decreased and surface air and soil temperatures increased; there was a noisy distribution of precipitation change with little mean change over the 13 months of the experiment.

Recently, Lean and Warrilow (1989) have reported briefly on a longer (3 year) experiment, with changes in land surface characteristics similar to those of Dickinson and Henderson-Sellers (1988); statistically significant reductions in rainfall were obtained in response to deforestation. A similarly clear response has been obtained by Shukla et al (1990) in a 1-year experiment. However, it is difficult from these experiments with changes in several land surface parameters to identify and analyse the impact of any one parameter. In this paper a series of simple experiments designed to test the response of a version of the UKMO 11-layer GCM to albedo increases in areas of tropical rainforest is described. It is envisaged that comparison with other work such as that of Potter et al. (1975) will contribute to our understanding of mechanisms of response in tropical latitudes to albedo modification.

2. The UK Meteorological Office 11-layer GCM

The 11 layer model is a primitive equation, global, finite difference GCM with a $2^1/_2 \times 3^3/_4°$ regular latitude - longitude grid. The model is as described by Slingo and Pearson (1987) except that i) albedos (discussed in section 4) vary geographically, ii) the longwave radiation scheme predates the changes described by Slingo and Wilderspin (1986), iii) surface resistance to evaporation of 60 sm^{-1} is not included and iv) cloud radiative properties are as described in Slingo (1985). A σ (= pressure/surface pressure) vertical co-ordinate system is employed. The atmospheric column is divided into 11 layers (Slingo, 1985). Finer σ co-ordinate resolution is used near and above the tropopause and in the lowest 3 layers ($\sigma < 0.79$) which are influenced by boundary layer processes.

The model is run with an interactive radiation scheme (Slingo, 1985), with both diurnal and annual solar cycles. Cloud is prescribed on a zonal average basis and updated every 5 days according to a composite of observed seasonal climatologies. Sea surface temperatures and sea-ice are prescribed every 5 model days by interpolation between monthly climatologies.

These experiments were integrated with a boundary layer scheme recommended by Clarke (1970). The main processes included in this scheme are discussed in detail by Carson (1982). A bulk Richardson number, R_{IB}, is derived as a measure of the stability of the lowest model layer as a function of the gradient of specific humidity and potential temperature between the surface and lowest model layer. The calculated value of R_{IB} is

used, in conjunction with a roughness length of 10 cm over land, to determine the bulk transfer coefficients for moisture, sensible heat and momentum. The surface flux of any parameter x is then given by

$$F_x = -C_x V_{(zi)} \Delta x_{(zi)} \qquad (1)$$

where C_x is the calculated transfer coefficient, $V_{(zi)}$ the wind velocity in the lowest model layer and $\Delta x_{(zi)}$ is the difference between the values of x at the surface and at a height Z_i. For soil moisture content (SMC) of less than 5 cm, the evaporation is reduced below the "potential" rate calculated assuming the surface to be saturated according to

$$\text{Evaporation} = \frac{\text{SMC}}{5} \times \text{potential evaporation}$$

A "bucket hydrology" is used to predict the SMC of the single soil layer. In the standard version of the model, rainfall and snowmelt are allowed to increment the SMC until it attains a value of 15 cm. Thereafter any further supply of moisture is assumed to runoff until evaporation again reduces the SMC to less than 15 cm. Run off plays no further role in the hydrological cycle of the model.

The surface vegetation and soil types used in this suite of experiments were derived by averaging the 1° latitude x 1° longitude Wilson and Henderson-Sellers (1985) data archive at the coarser model resolution in accordance with the technique suggested in their paper.

The albedo for any grid square was the weighted average of the albedo appropriate to the average vegetation type and the average soil colour. The weights were the percentage of the grid square covered by vegetation and bare soil respectively. The soil albedo was taken to be that of moist soil except in areas of desert and semi-desert where dry soil albedo values were used. The values calculated for the region of tropical forest in South America, discussed in this paper, are shown in Figure 1.

Fig 1 →

3. Model climate in the South American region

3.1 Introduction

The version of the Meteorological Office model used in these experiments was the so-called 'second annual cycle' version. The atmospheric simulation obtained with this model has been compared to observations by Ingram (1985) in an Internal Note (available on request). As noted by Ingram, the simulation is quite similar to that of the 'third annual cycle' version, for which a number of maps and cross-sections are shown by Slingo and Pearson (1987) (their 'control'). Although Slingo and Pearson obtained a considerably improved simulation in middle latitudes by including a parametrization of gravity wave drag, the tropical tropospheric simulation was little affected. Ingram found that in both northern winter and summer, with the $2^1/_2°$ by $3^3/_4°$ resolution used here, the zonally-averaged tropical zonal winds were less than 5 m/s different from the observed winds except in a region of the upper troposphere above 500 mb within 10° of the equator, where the model winds were too westerly. Tropical temperatures were mostly cooler than observed, by 0 to 2K in the middle troposphere, but locally up to 4K near 850 mb at 20-30°

latitude. Aspects of the simulations in the South American region are discussed in the following sections, with the main emphasis on the moisture cycle.

3.2 Sea level pressure

Ingram's maps show that, in the South American region, the sea level pressure patterns give a good simulation of the observed features with subtropical highs in both solstitial seasons in the south Atlantic and eastern Pacific and anticyclones near the observed latitudes north of the equator in the north Atlantic and east Pacific. The South American heat lows are close to the observed positions and intensities. Ingram shows errors to be less than 4 mb within 30° of the equator in the Atlantic sector, except over North Africa in December to February and parts of Brazil south of 15°S in June to August (both positive errors).

3.2.2 Precipitation and evaporation

Figure 2(a) shows the observed rainfall for southern summer according to Jaeger (1976). At this time of year, the ITCZ is in its southernmost position with rainfall exceeding 5 mm day^{-1} over much of 0-20°S, with maximum rainfall near 10°S over the Amazon basin. Rainfall is light over Venezuela and the Nordeste region of Brazil. The model experiment with realistic albedos (Figure 2(b)) simulates this distribution well though the maximum is rather weak and too far southeast. During southern autumn, the rainbelt begins to move north, crossing the equator early in May (see Jaeger, 1976). Figure 5 shows that the model behaves similarly, though the maximum is at the equator

in April. By this time, the model's southern maximum near 15°S has disappeared. The autumn mean maps in Figure 3b again show the simulation to be very realistic except that the minimum near 10-15°S over eastern Brazil is too strong and the area with more than 5 mm day^{-1} has extended too quickly northward west of 60°W. The dry area (less than 2 mm day^{-1}) south of 5°S in May in the 75°-52$^1/_2$°W means (Figure 5) extends north to the equator by July when the model's rainfall maximum is located over the ocean. These northward shifts are less marked in Jaeger's estimate of the observed (Figure 4(a)) which still has the maximum over the land in the June-August mean. At this time, the model has an intense peak over the Atlantic near 45°W for which there is little observational evidence. However, the observed southern edge of the rainbelt is close to the modelled over much of eastern Brazil though further south by several degrees near 70°W. Summarizing, the simulated rainfall during the nine months of the experiments is generally quite realistic apart from the tendency for the rainbelt to move too far north in northern summer.

Fig 5

In the model, the reduction in soil moisture caused by the cessation of the rains south of the equator around May leads to a reduction in evaporation. In the rainy regions, evaporation is between 4 and 5.5 mm/day (Figure 6), but in May this falls to below 2 mm day^{-1} south of 7$^1/_2$°S, and values at 1$^1/_4$°S average as low as this over 52$^1/_2$-75°W by August, with less than 1 mm day^{-1} south of 5°S. The seasonal variation of these rates is excessive, generating minimum values which are small compared with the 3-4 mm day^{-1} evaporation rates observed throughout the year at Manaus by Shuttleworth (1988). The wet season evaporation is too large because of the absence of a stomatal resistance. It is possible that in reality larger moisture

storage than the model's 15 cm, associated with swamp and other wet areas in the Amazon basin, allow evaporation to continue at potential evaporation levels for longer than in the model and by feedback on the atmospheric moisture balance lead to a lesser decrease of rainfall in the southern winter south of the equator. Experiments with increased moisture storage parallel to the present experiments showed some evidence to support this speculation (Wilson, 1984).

The interactions between the hydrological cycle and surface temperature are illustrated by Figure 7 for the 75-52$^1/_2$°W averages at 8$^3/_4$ and 3$^3/_4$°S. The declines in soil moisture which follow the northward transfer of the rainbelt in southern autumn are associated with rises in surface temperature of about 5K from April or May to August, the converse of what might be expected from the changes in solar declination, at least up to July. Some warming is observed in reality, though generally not so large (eg 1.5K at Manaus at 3°S 60°W (Shuttleworth, 1988)).

3.2.3 Tropospheric winds

The 850 mb and 250 mb winds have been compared to averaged analyses from the Meteorological Office operational forecast archives for June 1983-May 1986. For reasons of space, illustrations are omitted. The prevailing easterlies at 850 mb over the tropical Atlantic and much of South America were well simulated in all three seasons, with intensities of up to 10 m/s as observed; flow near the Andes differed in detail, with too much flow across the mountains in some latitudes, presumably because of an underestimation of mountain elevations. At 250 mb, the weak easterly flow observed over tropical

South America in southern summer and autumn tended to be westerly in the model. The winter (June-August) simulation had easterly flow as observed. The locations and strengths of the subtropical jets and the gradients on their equatorward sides were generally well simulated.

4. Experiment design

The experiments to be compared in this paper are listed in Table III; they differ only in the albedos. Expt 2 is the 'second annual cycle' experiment referred to in section 3. It has albedos of 0.2 over all snowfree land. Expt F (Forest) has snowfree albedos dependent on the vegetation and soil datasets described by Wilson (1984). For tropical forests and woodland, these albedos are between 0.12 and 0.15, depending on the type of forest or woodland and, for woodland where some soil is exposed, on the soil albedo. In Expt G (Grassland), the tropical forest albedos were replaced by values appropriate for grassland. These grassland albedos are between 0.18 and 0.22, depending on the soil type. (In prescribing the soil colour distribution, light rather than medium coloured soil was specified erroneously at a few points in Amazonia. This made the grassland albedo at these points 0.03 higher than intended. However, grassland albedo can be higher than 0.22 so that this error in no way invalidates the results).

As well as using the differences between experiments G and F (called (G-F)) to assess the effects of deforestation, we shall also examine the differences between experiments 2 and F ((2-F)). Since the grassland albedos are close to 0.2, the local albedo forcings in (2-F) and (G-F) are clearly similar (Figure 8). It is of course possible that the remote effects of changes in albedo outside the tropical forest regions will have

an impact on the (2-F) differences. This applies particularly to the differences over the rest of South America. These are predominantly of the same sign as the forest changes, since the albedos there are between 0.15 and 0.21 in Expt F and G. Thus Expt (2-F) may be regarded as a somewhat larger scale vegetation change experiment for South America. Changes elsewhere may also have remote effects over South America, but these appear to be small. Similarly, the effects of the deforestation of tropical Africa and southeast Asia in Expt (G-F) also appear to be small over South America and certainly dominated by the local forcing.

Expt 2 was run from observed data for 25 July 1979 for a period of eight years. However, the means used here are, except where otherwise stated, for the period of nine months starting from December of the first year. Expts F and G were initialised from 1 December of the first year of Expt 2, and run for nine months.

5. Results

5.1 Mechanisms

The albedo increases imposed in the experiments in areas of tropical forest varied from 0.04 to 0.10. Potential consequent impacts (discussed earlier in section 1) are summarized in Figure 9. With incoming surface solar radiation of up to 300 Wm^{-2} this could reduce the absorbed solar radiation by up to 30 Wm^{-2} (Process A). If net surface longwave radiation remains unchanged there is less energy available for latent or sensible heat flux from the surface and for transfer into the ground. Secondary effects that may arise include (i) a decrease in evaporation (process B) arising directly from the

reduction in available energy, and (ii) the decrease in precipitation resulting from this (process C). There is also the important feedback from the decrease in net radiative heating of the total (atmosphere + surface) column. This leads (Charney, 1975) to a reduction in ascent (process D), moisture convergence and rainfall (process E). This must over a period of time lead to changes in the moisture budget and hence soil moisture content (process F). Each of these processes has been identified in previous modelling experiments (section 1). If the decrease in precipitation exceeds that in evaporation, drying out of the soil occurs, thus promoting a further decrease in evaporation (process G) and this may lead to an increase in sensible heat flux and surface temperature despite the increase in albedo. In contrast the combined impact of processes B and G may be sufficient to cause a larger decrease in evaporation than in precipitation. This results in a negative feedback (process H) tending to increase soil moisture content.

5.2 Quantitative impacts

(a) Area means

To obtain a broad quantitative assessment of the impact of the albedo changes, the differences between the high and low albedo cases were averaged over the region 5°N-15°S, $52^1/_2$°-75°W, for each month of the integration. Results for experiments (G-F) and (2-F) are given in Table IV. In both cases considerable decreases in precipitation occurred especially in the first four months, with the larger decreases in (2-F). Larger changes are to be expected in (2-F) because of the more extensive albedo changes; these are evident from

the changes in the total turbulent heat flux, which apart from changes of order 1 Wm^{-2} in soil heat storage, equal the changes in net radiation. After the first month, these changes are about 20% larger in (2-F) over the deforested area as approximated by the averaging region. Changes over parts of South America outside the deforested area, where albedos are unchanged in (G-F), but generally increased in (2-F), may also contribute to the greater rainfall changes in (2-F). The area averaged changes in rainfall are smaller in the final season (June, July, August) at least partly because in this season the main rain belt is north of the deforested region (Figure 4 (b)).

During the first two seasons, the rainfall in (G-F) is decreased over most of the deforested area (Figure 10 (a,d)), with local differences of up to 5 mm/day. The results in (2-F) (Figure 10 (b,e)) are generally similar, though the differences extend less far east in (G-F), as would be expected in view of the more limited extent of the albedo increases (Figure 8a). Near 10°S in December to February (DJF) there are decreases in rainfall over parts of the deforested area east of about 60°W. There is a similar feature in March-May (MAM), which is also present in (2-F). Since the control experiment (Expt 2) was run for 8 years in this case, it is possible to assess the statistical significance of these results using Student's t-test (Figure 10 (c, f)). It may be noted that the zero lines in Figure 10 (b) and (c) are different (also in Figure 10 (e, f) and (h,i)); this is because the 8-year mean, rather than just one year's values, is subtracted from Exp F in the t-tests. A large part of the South American differences between 5°N and 15°S in (2-F) are found to be significant at the 10% level (5% on a one-tailed test, whose use is justified here since we would expect decreases with

increased albedo as discussed in sections 1 and 5). It is not possible to comment on the significance of the increases over eastern Brazil in DJF because they do not occur in (2-F); a small part of the similar increases in MAM are significant at the 10% level.

The area of significant decreases extends southeast of the main region of decreases in both these seasons in (2-F); the presence of a similar pattern in (G-F) indicates that in (2-F) this change is due to the albedo increases in the deforested area rather than those further south. This implies that the tongue of heavy rainfall obtained in the model extending southeast from Amazonia owes its existence at least in part to the Amazonian rainfall region. This tongue is not a model artefact, being evident in the Jaeger climatology in DJF (Figure 2(a)) and also to a lesser extent in MAM (Figure 3(a)). In Figure 2(a), the extension over the ocean is only weakly defined; it is more obvious in the satellite cloud patterns of Miller and Feddes (1971). A feature similar to but stronger than this South American tongue is the South Pacific Convergence Zone which is prominent throughout the year extending southeast from near 10°S 160°E towards southern South America both in the model and in Jaeger's climatology (Figures 2 to 4). This feature is observed to respond to eastward displacements of the equatorial Pacific convergence region in association with the El Nino/Southern Oscillation phenomenon. It is therefore not surprising that its South American counterpart should respond to variations in the intensity of Amazonian rainfall.

Apart from the extension of this tongue over the south Atlantic, the changes in rainfall are mostly limited to the land in DJF; however in MAM the decreases over northern South America extend eastward over

the equatorial Atlantic, with increases to the north, both in (G-F) and (2-F). The t-tests for (2-F) show only limited significance for the decreases, rather more for the increases. The similarity of the patterns over the Atlantic in (G-F) and (2-F) is quite surprising since there are large albedo decreases over North Africa in (2-F) which are not included in (G-F); the two experiments have similar albedo increases over the African tropical forests.

In June - August (JJA), changes are small south of the equator in both (G-F) and (2-F), as expected from the low rainfall at this season. Both have general decreases north of the equator which are larger in (2-F). Again, this is likely to be due to the more extensive albedo increases in that experiment; these average about 0.03 over the parts of northern South America outside the tropical forest region. The decreases in (2-F) are significant, both over South America north of the equator and also over parts of the northern tropical Atlantic. However, the decreases over the ocean are weaker in (G-F) than in (2-F).

(b) Changes in moisture convergence and flow patterns

Average decreases occurred in moisture convergence (P-E) for both experiments in most months (Table IV) although again the response was larger in (2-F). This deficit is associated with decreases in both rainfall and evaporation with the decrease in precipitation generally exceeding that in evaporation. This indicates that the decrease in precipitation results from a combination of reductions in moisture convergence and evaporation. A similar result has been obtained for previous albedo change experiments (see Table I).

From December to March, particularly in the west of the basin, decreases in precipitation are coincident with decreases in moisture convergence (not shown). Decreases in (P-E) are for the most part 1-2 mmd^{-1} where albedo was increased west of 60°W.

(c) Changes in turbulent heat flux and surface temperature

Changes in evaporation (Table IV) are of a similar nature to those in precipitation. There are average decreases of 0.5 to 1 mm day^{-1} in the first 5-7 months with smaller changes later. Area-averaged soil moisture content was smaller throughout the first 7 months of integrations with higher albedo (Table IV). This is to be expected with decreases in (P-E). Decreases are largest in February-March-April when the greatest fraction of the basin is influenced by precipitation changes.

As anticipated in section 5.1 the decrease in evaporation is a response to a reduction in absorbed energy at the surface and also to increased surface resistance to evaporation. This greater resistance occurs where the decrease in (P-E) reduces the soil moisture (feedback process F in Figure 9).

In December and January small decreases of up to 2.0 mm day^{-1} can be seen in time-latitude diagrams of changes in evaporation. (Figures 11 and 12).

In (G-F) latitude averaged decreases peak at up to 1.6 mm day^{-1} (- 45 Wm^{-2}) between $2^1/_2$°N and 5°S in December/January/February and May and between 10° and 15°S in March and April. (2-F) shows similar results.

Surface temperature and sensible heat flux display predominantly small basin average increases in the first six months (Table IV); there are decreases in the last three months of the study period, when the hydrological changes which have earlier maintained higher temperatures become weak. The increases in temperature and sensible heat flux are more pronounced in (2-F) (Table IV). On a seasonal basis the extent of the region of moisture restricted evaporation is marginally greater in the integrations with higher albedo and the onset date slightly earlier. Consequently by the final 3 months similar hydrological restrictions on evaporation occur in both control and perturbation experiments. Process G (Figure 9), by which increases in surface temperature and sensible heat flux are forced by enhanced hydrological feedback diminishes in importance.

Locally, process G is responsible for considerable changes in the early months of the experiment. For example, in December and January in the north-west of the Amazon region many points have an increased surface resistance because of reduced soil moisture due to the decrease in P-E; consequently evaporation decreases of between 1 and 2 mm day^{-1} (30-60 Wm^{-2}) occur. There are corresponding increases of 10-30 Wm^{-2} in sensible heat flux, and a surface warming of between 2.5K and 5.0K.

The responses of the surface temperature and total turbulent heat flux fields result from complex interactions between components of the surface heat and energy balances. Basin average changes (Table IV) show decreases every month in total turbulent heat flux. Decreases of up to 20 Wm^{-2} occur in the first few months and smaller decreases of 10 to 15 Wm^{-2} in the last few months when incoming solar radiation is less and evaporative reductions, surface warming and longwave radiation losses are smaller.

Summary

General circulation models have been shown to be sensitive to surface albedo. The mechanisms of response and sensitivity of the UK Meteorological Office 11-layer general circulation model to albedo increases of the magnitude associated with deforestation in Amazonia have been examined. The results of this study are qualitatively similar to those of other studies using a wide range of GCMs. Statistically significant decreases in precipitation occur within Amazonia, and to the southeast in December-February and March-May. Surface fluxes of moisture and sensible heat and surface temperature respond both to the reduction in absorbed energy and the redistribution of this energy between sensible and latent heat flux in response to changes in moisture-limited evaporation.

Acknowledgements

Much of the initial research for this paper was carried out whilst M F Mylne (then M F Wilson) was supported by a NERC CASE studentship in conjunction with Liverpool University and the UK Met. Office.

List of Figures

List of Tables

Table IV Differences in mean monthly values of selected variables between experiments with high and lower albedo in Amazonia,

a) G-F

b) 2-F

Table I

Effects of albedo modification in GCM sensitivity experiments

Experiment	Increase in Albedo	Change in Evaporation(E) ($mmday^{-1}$)	Change in Rainfall(P) ($mmday^{-1}$)	% Change in P / Albedo Change
Charney et al. (1977)				
Sahel	.21	-0.9	-3.4	-2.2
NW India	.21	-0.5	-2.6	-2.5
Great Plains	.21	-1.0	-1.5	-2.0
Central Africa	.21	-0.7	-3.1	-3.0
Bangladesh	.21	-0.2	0	0
Mississippi	.21	-1.6	-1.1	-1.2
Chervin (1979)				
Sahara	.22		-2.5	-1.8
W USA	.33		-1.0	-0.5
Sud and Fennessy (1982)				
Sahel	.12	-0.7	-1.5	-2.1
NW India	.15	-0.2	-0.5	-0.9
NE Brazil	.21	-0.3	-0.5	-1.1
Great Plains	.17	-0.2	0	0.1

Planton (1986)

Sahara summer	.10	-0.15	-0.20
(31°N) winter	.10	-0.06	-0.08
Sahel summer	.10	-0.08	-0.30
(22°N) winter	.10	-0.08	-0.15

Carson and Sangster (1982)

Global	0.2	-0.95	-1.22	-1.3

Table II

Effects of perturbation of surface moisture in GCM sensitivity experiments

Reference	Area	Change in β	Major changes in precipitation
Kurbatkin et al. 1979	All land	Model generated soil moisture to dry ie β=0	Decrease mostly < 1 $mmday^{-1}$ large decrease up to 5 $mmday^{-1}$ over parts of India Increase east coast Asia and adjacent ocean, southern USA and equatorial Indian Ocean. Largest increase 1 to ~5 $mmday^{-1}$ Colombia and equatorial west Pacific.
Shukla and Mintz 1982	All land	Decrease β=1 to β=0	Decrease generally ~25%. 3-4 $mmday^{-1}$ decrease over Africa. Little change in South America due to increased moisture convergence. Slight increase south east Asia.
Rowntree and Bolton 1983	Much of Europe	Initial β=1 to β=0 (also variable β)	Large decreases after a few days which spread to adjacent areas. Less persistent with westerly winds.

Suarez and Arakawa (Reported in Mintz, 1984)	All land	Decrease $\beta=1$ to $\beta=0$	-100% reduction in precipitation over land initially and maintained over many areas.
Sud and Fennessy 1984	Sahel Thar desert NE Brazil Great plains	) Interactive) soil moisture) to dry ie) $\beta=0$	Increase 0.36 $mmday^{-1}$ Increase 2.67 $mmday^{-1}$ Decrease 0.31 $mmday^{-1}$ Increase 0.18 $mmday^{-1}$
Carson and Sangster 1982	All land	Initial $\beta=1$ to initial $\beta=0$	Average decrease 1.23 $mmday^{-1}$ day 21 to 50 Average decrease 0.39 $mmday^{-1}$ day 171 to 200
Cunnington and Rowntree 1986	Africa North of 10°N	$\beta=1$ to initial $\beta=0$	Decrease ~50% (3 $mmday^{-1}$)
Yeh et al. 1984	30°N-60°N	$\beta<1$ to $\beta=1$	Increase by up to 4 $mmday^{-1}$) increases
	0-30°N		Increase ~0.5 $mmday^{-1}$) persist
	15°S-15°N		Increase 0.5 to 2.5 $mmday^{-1}$)-3 months

Table III

Experiments discussed in assessing the impact of albedo change in Amazonia

	Snow free albedos	
Experiment name	Tropical forests	Other land
Expt 2	0.2	0.2
Expt F	Forest albedo (0.12-0.15)	Vegetation dependent (0.12-0.35)
Expt G	Grassland albedo (0.18-0.22)	As expt F

Table IV

Differences in mean monthly values of selected variables between experiments with grassland and forest albedo in Amazonia (Grassland-Forest)

a) G-F

Variable	Month									
	D	J	F	M	A	M	J	J	A	AV
RL ($mmday^{-1}$)	-0.04	-0.11	-0.05	-0.12	0.08	-0.10	-0.02	0.23	0.05	-0.01
RC ($mmday^{-1}$)	-1.35	-1.21	-0.65	-2.25	-0.77	-1.44	-0.36	-0.03	-0.19	-0.92
Total P ($mmday^{-1}$)	-1.39	-1.32	-0.70	-2.37	-0.69	-1.54	-0.38	0.20	-0.14	-0.93
Evap ($mmday^{-1}$)	-0.64	-0.70	-0.73	-0.82	-0.71	-0.43	-0.37	0.03	-0.02	-0.49
(P-E) $mmday^{-1}$	-0.75	-0.62	0.03	-1.55	0.02	-1.11	-0.01	0.17	-0.12	-0.44
Soil moisture (cm)	-0.60	-1.69	-1.26	-1.60	-1.08	-0.84	-0.44	0.34	0.12	-0.78
Surface T (°C)	0.08	0.36	0.38	0.19	-0.04	0.34	0.05	-1.78	-0.55	-0.11
SH (Wm^{-2})	- 3.0	5.2	5.7	7.6	5.9	0.1	-1.0	-11.4	-9.9	0.6
SH + LE (Wm^{-2})	--15.0	-15.0	-15.3	-16.0	-14.5	-12.3	-9.7	-10.5	-10.5	-13.2

RL = Large scale rainfall

RC = Convective rainfall

Total P = Total precipitation

P-E = Precipitation - Evaporation

Surface T = Surface temperature

SH = Sensible heat flux

SH + LE = Sensible heat and latent heat flux ie total turbulent heat flux

b) 2-F

Variable	Month									
	D	J	F	M	A	M	J	J	A	AV
RL ($mmday^{-1}$)	-0.005	-0.22	-0.06	-0.19	-0.06	-0.10	-0.09	0.08	-0.004	-0.07
Rc ($mmday^{-1}$)	-1.38	-2.87	-2.28	-3.54	-1.19	-0.97	-0.54	-0.18	-0.19	-1.46
Total P ($mmday^{-1}$)	-1.39	-3.09	-2.34	-3.74	-1.24	-1.07	-0.63	-0.10	-0.20	-1.53
Evap ($mmday^{-1}$	-0.56	-0.96	-1.13	-0.10	-1.21	-0.68	-0.50	-0.29	-0.32	-0.74
(P-E) $mmday^{-1}$	-0.82	-2.13	-1.21	-2.74	-0.04	-0.39	-0.14	0.19	0.12	-0.80
Soil moisture (cm)	-0.23	-1.87	-3.10	-4.23	-2.81	-1.73	-0.67	-0.15	0.13	-1.63
Surface T (°C)	-0.06	0.74	1.19	0.69	1.49	0.72	-0.16	-1.24	-0.91	0.27
SH (Wm^{-2})	1.7	9.6	13.5	10.6	16.3	4.8	-0.1	-4.8	-4.2	5.2
SH + LE (Wm^{-2})	-14.5	-18.0	-19.1	-18.1	-18.4	-14.7	-14.4	-13.0	-13.4	-16.0

References

Carson, D.: 1982, Current parameterization of land-surface processes in atmospheric general circulation models. In land surface processes in atmospheric general circulation models (ed) Eagleson, P S, Cambridge University Press 67-108.

Carson, D. and Sangster, A., 1982, The influence of land surface albedo and soil moisture on general circulation model simulations, Numerical Programme Rep 2 P5.14-5.21 UK Meteorological Office, Bracknell Berks.

Charney, J. G.: 1975, Dynamics of deserts and drought in the Sahel. Quart J Roy Meteor Soc 101 193-202.

Charney, J G, Quirk, W.J, Chew, S.M. and Kornfield, J.: 1977, A comparative study of the effects of albedo change on drought in semi-arid regions. J Atmos Sci 34 1360-1388.

Chervin R.M.: 1979, Response of the NCAR general circulation model to changed land surface albedo. Report of the JOC study conference on climate models: performance, Intercomparison and sensitivity studies, Vol 1, 563-581.

Clarke, R.H.: 1970, Recommended methods for the treatment of the boundary layer in numerical models. Aust Met Mag 18, 51-73.

Cunnington, W.M. and Rowntree, P.R.: 1986, Simulations of the Saharan atmosphere dependence on moisture and albedo. Quart J Roy Meteor Soc 112 971-999.

Dickinson, R.E. and Henderson-Sellers, A.: 1988, Modelling tropical deforestation: a study of GCM wind-surface parameterization. Quart J Roy Meteor Soc 114 439-462.

Henderson-Sellers, A. and Gornitz, V.: 1984, Possible Climatic impacts of land cover transformation, with particular emphasis on tropical deforestation. Climatic Change 6 231-257.

Henderson-Sellers, A. and Wilson, M.F.: 1983, Surface albedo data for climatic modelling. Rev. Geoph. Space Phys. 21 1743-1778.

Ingram, W.J.: 1985, A comparison of the time mean fields of the AGCM with observational data. Meteorological Office, Met O 20 Internal note 42

Jaeger, L.: 1976, Monatskarten des Niederschlags Für die ganze Erde. Bericht Deutsche Wetterdienst, 18, No 139.

Kurbatkin, G.P.: Manabe, S. and Hahn, D.G.: 1979, The moisture content of the continents and the intensity of the summer Monsoon circulation. Soviet Meteorology and Hydrology, 11, 1-6.

Lean, J. and Warrilow, D.A.: 1989, Simulation of the regional impact of Amazon deforestation. Nature. 342 411-413.

Miller, D.B. and Feddes, R.G.: 1971, Global atlas of relative cloud cover 1967-1970. Based on photographic signals from meteorological satellites, US Dept of Commerce, NOAA/USAF Air Weath. Service, ETAC, Washington, D.C.

Mintz, Y.: 1984, The sensitivity of numerically simulated climates to land surface boundary conditions. In Global climate (ed) J T Houghton, 79-105. Cambridge University press.

Planton S.: 1986, Sensitivity of the annual cycle simulated by a GCM to change in land surface albedo. Noordwijk: ESA SP-248 135-142.

Poore, D.: 1976, The values of tropical moist forest ecosystems and the environmental consequences of their removal. Unasylva 28 127-145.

Potter, G.L., Elsasser, H.W., MacCraken, M.C. and Luther, F.M.: 1975, Possible impact of tropical deforestation. Nature 258 697-698.

Rowntree, P.R.: 1988, Review of general circulation models as a basis for predicting the effects of vegetation change on climate. In Forests, climate and hydrology - regional impacts (Ed. E.R.C. Reynolds and F.B. Thompson) Proceedings of United Nations University Workshop, Oxford, March 1984, pp 162-193.

Rowntree, P.R. and Bolton, J.A.: 1983, Simulation of the atmospheric response to soil moisture anomalies over Europe. Quart. J. Roy. Meteor. Soc. 109 501-526.

Salati, E. and Vose, P.B.: 1983, Depletion of tropical rain forests. Ambio 12 67-71.

Shukla, J. and Mintz, Y.: 1982, Influence of land-surface evapotranspiration on the earth climate, Science, 215 1498-1501.

Shukla, J., Nobre, C. and Sellers, P.: 1990, Amazon deforestation and climate change. Science, 247, 1322-1325.

Shuttleworth, J.W.: 1988, Evaporation from the Amazon rain forest. Proc Royal Soc of London B 233 321-346.

Slingo, A.: 1985, Handbook of the Meteorological Office 11-layer atmospheric general circulation model. Volume 1: Model description. Dynamical Climatology Technical Note DCTN 29, Meteorological Office, Bracknell, UK.

Slingo, A. and Pearson, D.W.: 1987, A comparison of the impact of an envelope orography and of a parameterization of orographic gravity wave drag model simulations. Quart J Roy Meteor Soc, 113. 847-870.

Slingo, A. and Wilderspin, R.C.: 1986, Development of a revised longwave radiation scheme for an atmospheric general circulation model. Quart J Roy Met Soc 112, 371-386.

Sud, Y.C. and Fennessy, M.: 1982, A study of the influence of surface albedo on July circulation in semi and regions using the GLAS GCM, J Clim 2 105-125.

Sud, Y.C. and Fennessy, M.: 1984, A numerical study of the influence of evaporation in semi-arid regions on the July circulation. J Clim 4 383-398.

Wilson, M.F.: 1984, The construction and use of land surface information in a general circulation climate model. PhD thesis, University of Liverpool.

Wilson, M.F. and Henderson-Sellers A.: 1985, A global archive of land cover and soils data for use in general circulation climate models. J Clim 5 119-143.

Yeh T.C.: Wetherald, R.T. and Manabe, S.: 1984, The effect of soil moisture on the short term climate and hydrology change - A numerical experiment. Mon Weather Rev 112 474-490.

Figure 1

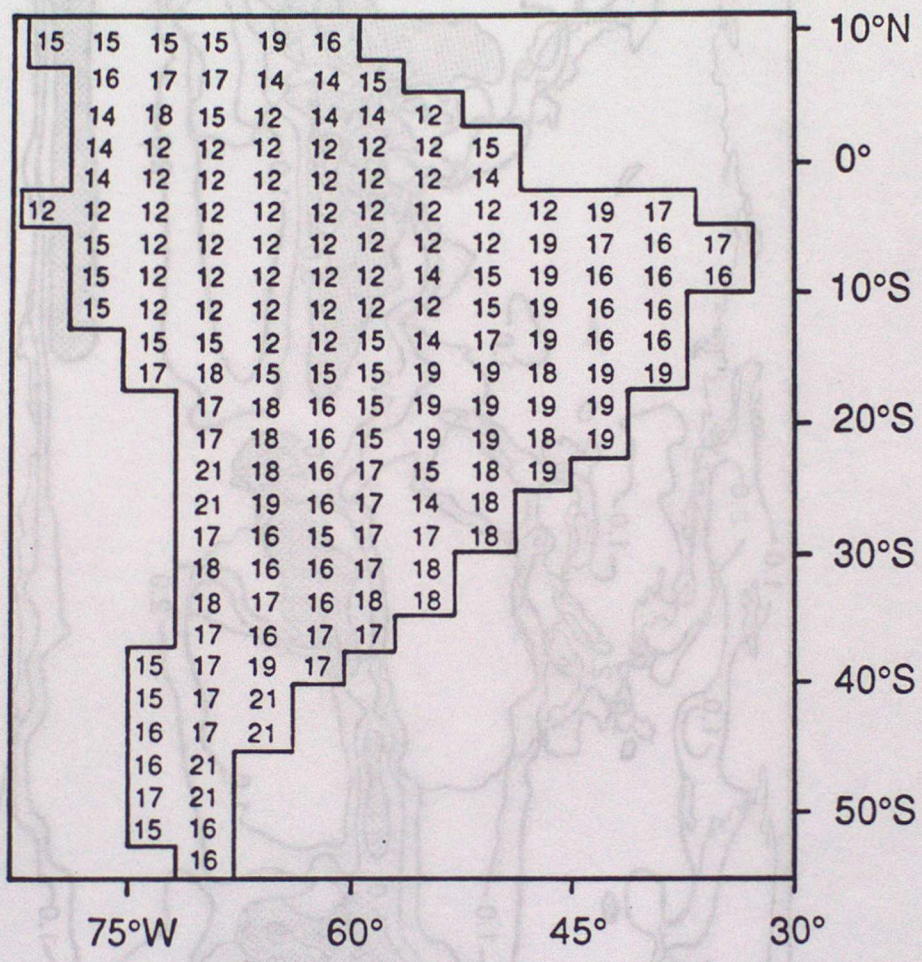
15 15 15 15 19 16
16 17 17 14 14 15
14 18 15 12 14 14 12
14 12 12 12 12 12 12 15
14 12 12 12 12 12 12 14
12 12 12 12 12 12 12 12 12 19 17
15 12 12 12 12 12 12 12 19 17 16 17
15 12 12 12 12 12 14 15 19 16 16 16
15 12 12 12 12 12 12 15 19 16 16
15 15 12 12 15 14 17 19 16 16
17 18 15 15 15 19 19 18 19 19
17 18 16 15 19 19 19 19
17 18 16 15 19 19 18 19
21 18 16 17 15 18 19
21 19 16 17 14 18
17 16 15 17 17 18
18 16 16 17 18
18 17 16 18 18
17 16 17 17
15 17 19 17
15 17 21
16 17 21
16 21
17 21
15 16
16
10°N
0°
10°S
20°S
30°S
40°S
50°S
75°W
60°
45°
30°

Figure 2a

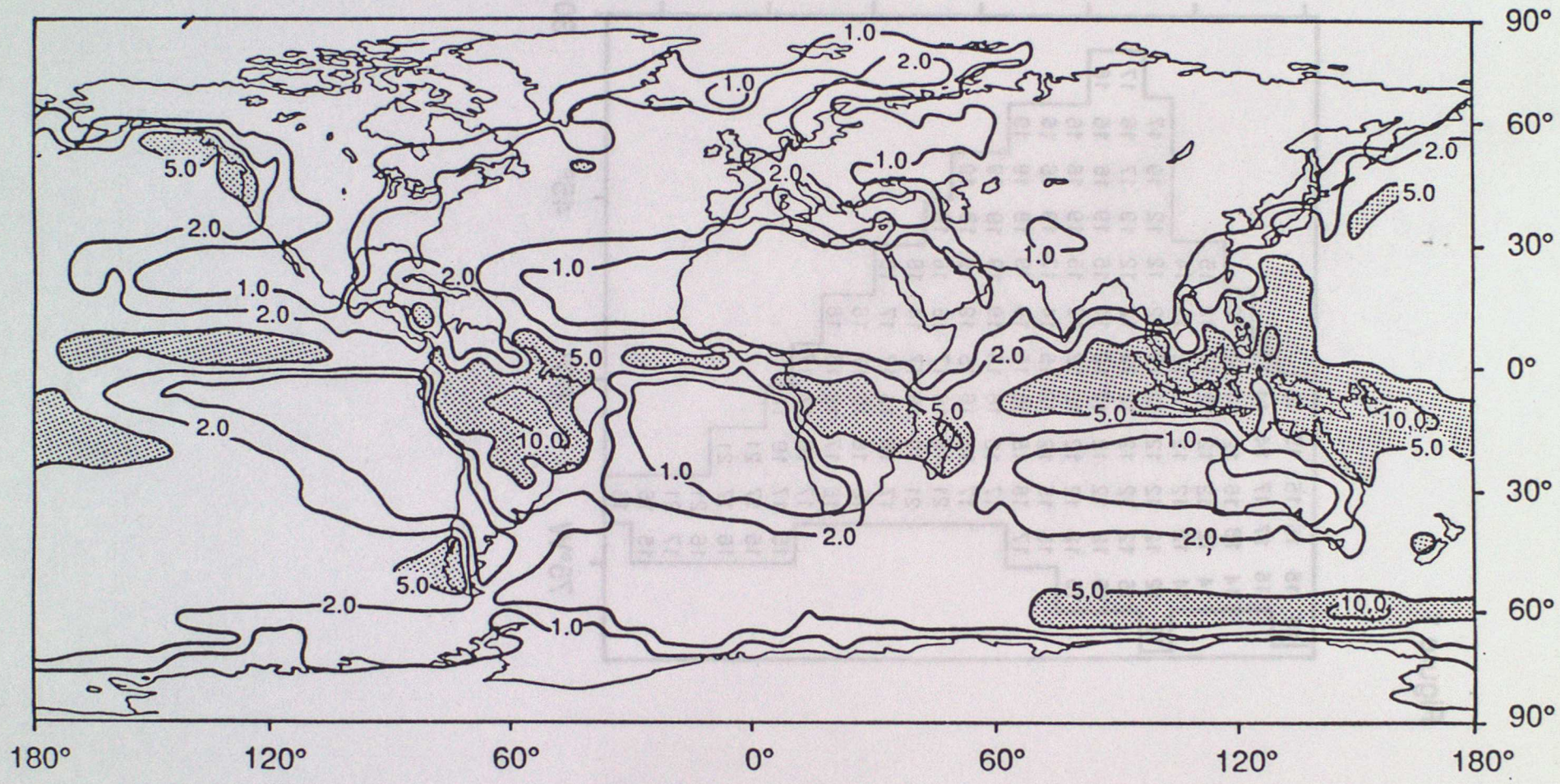

Figure 2b

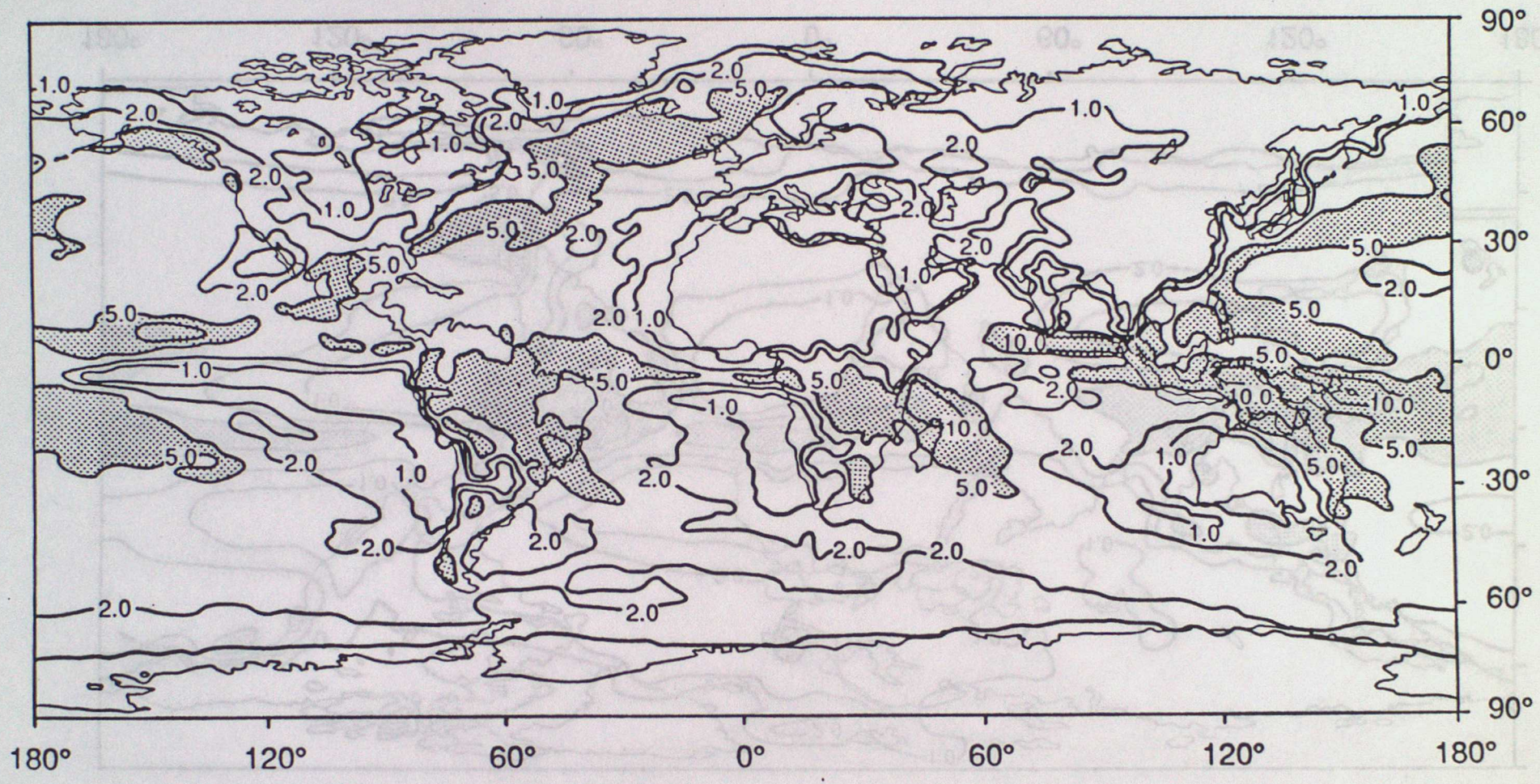

Figure 3a

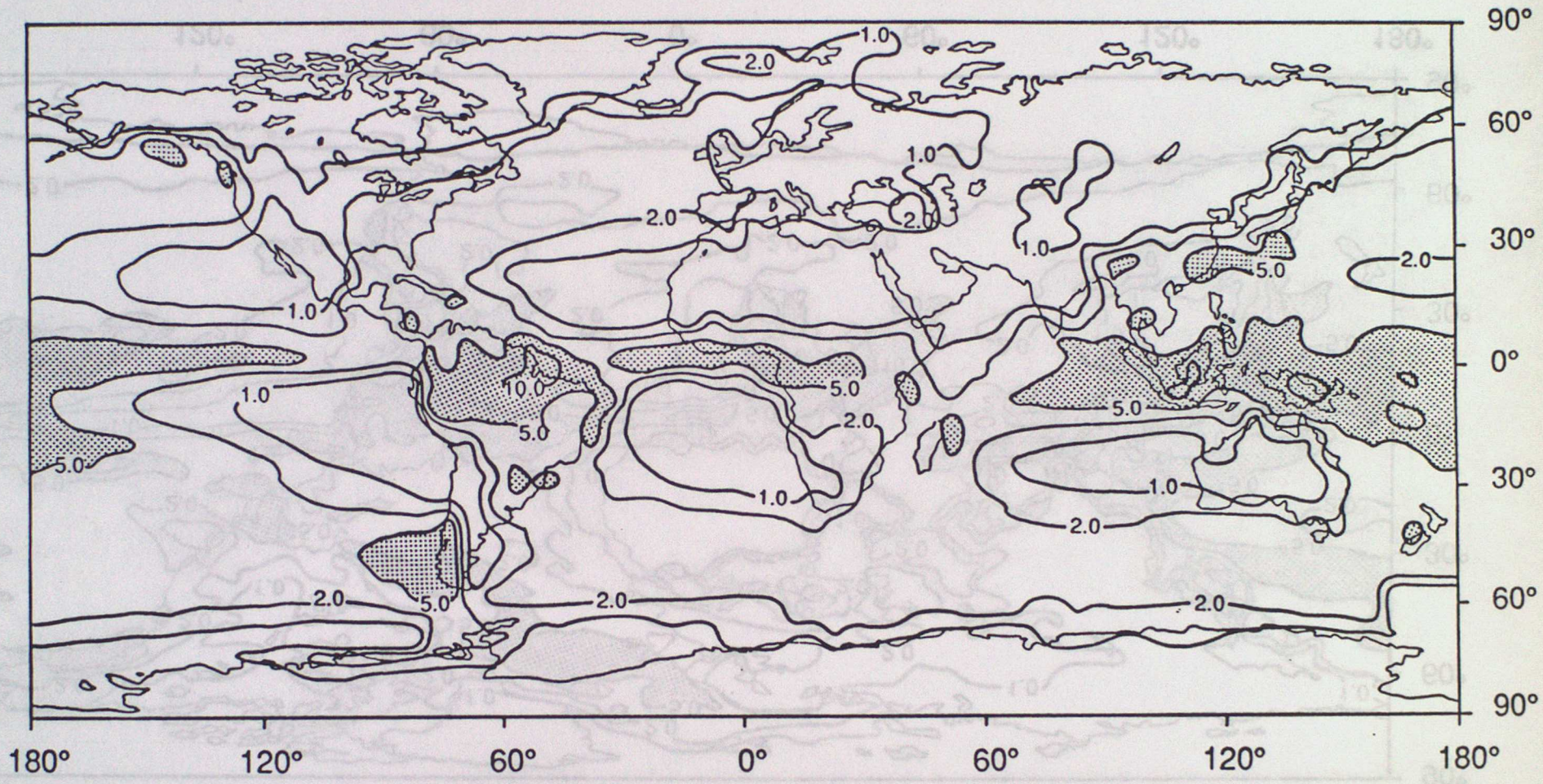

Figure 3b

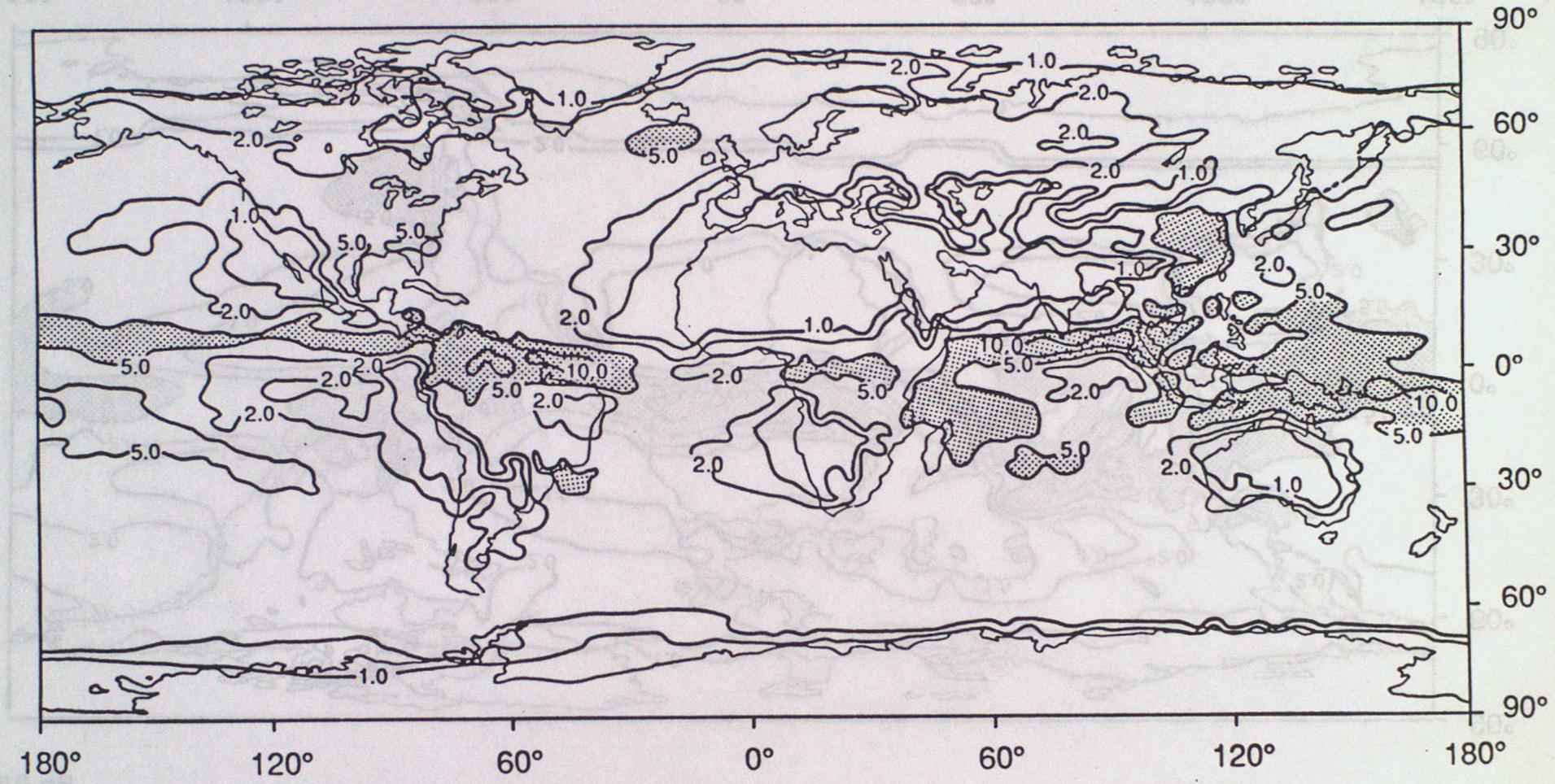

Figure 4a

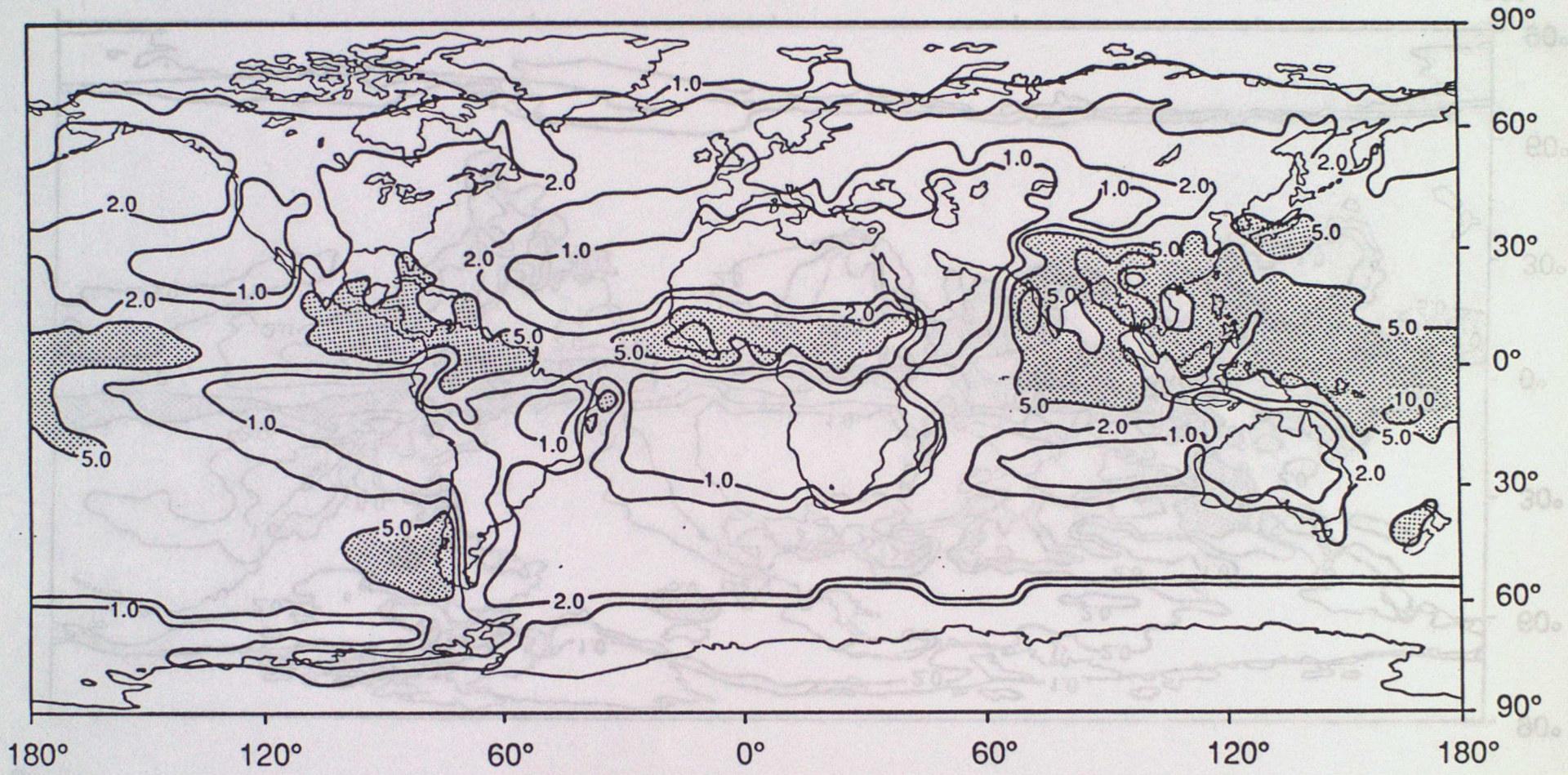

Figure 4b

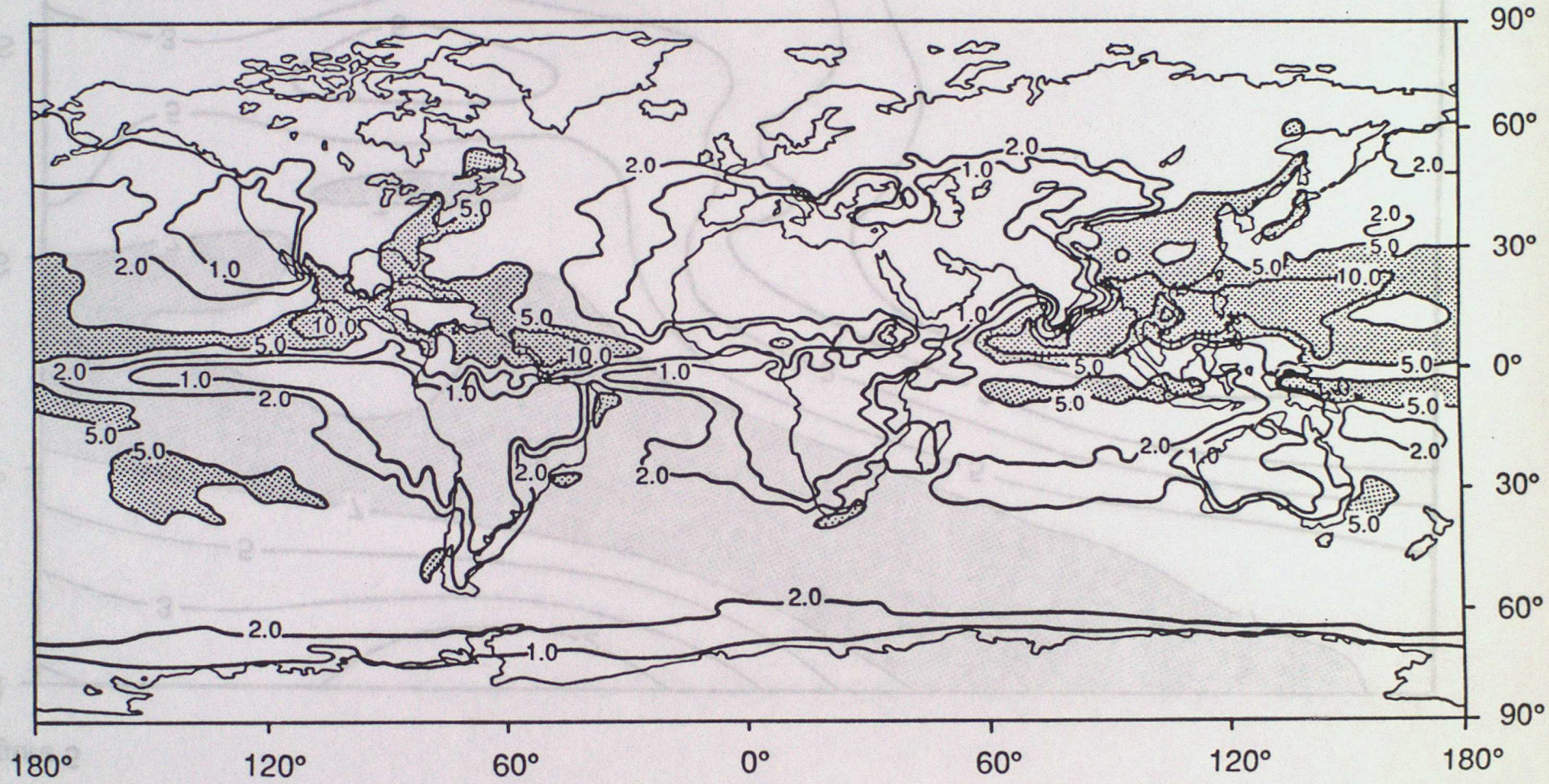

Figure 5

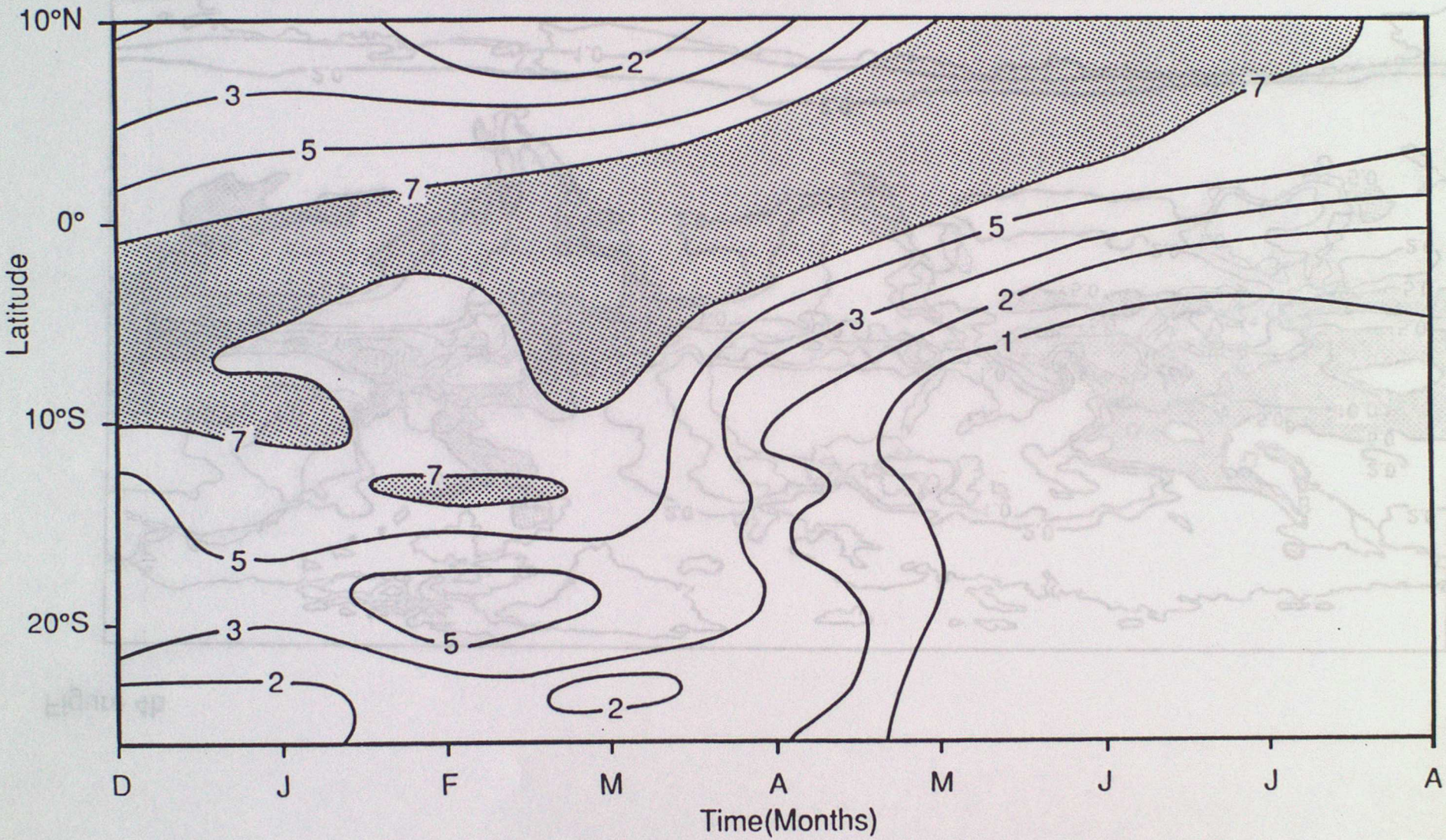
10°N
0°
10°S
20°S
Latitude
2
3
5
7
7
5
3
2
1
7
7
5
3
5
2
2
D
J
F
M
A
M
J
J
A
Time(Months)

Figure 6

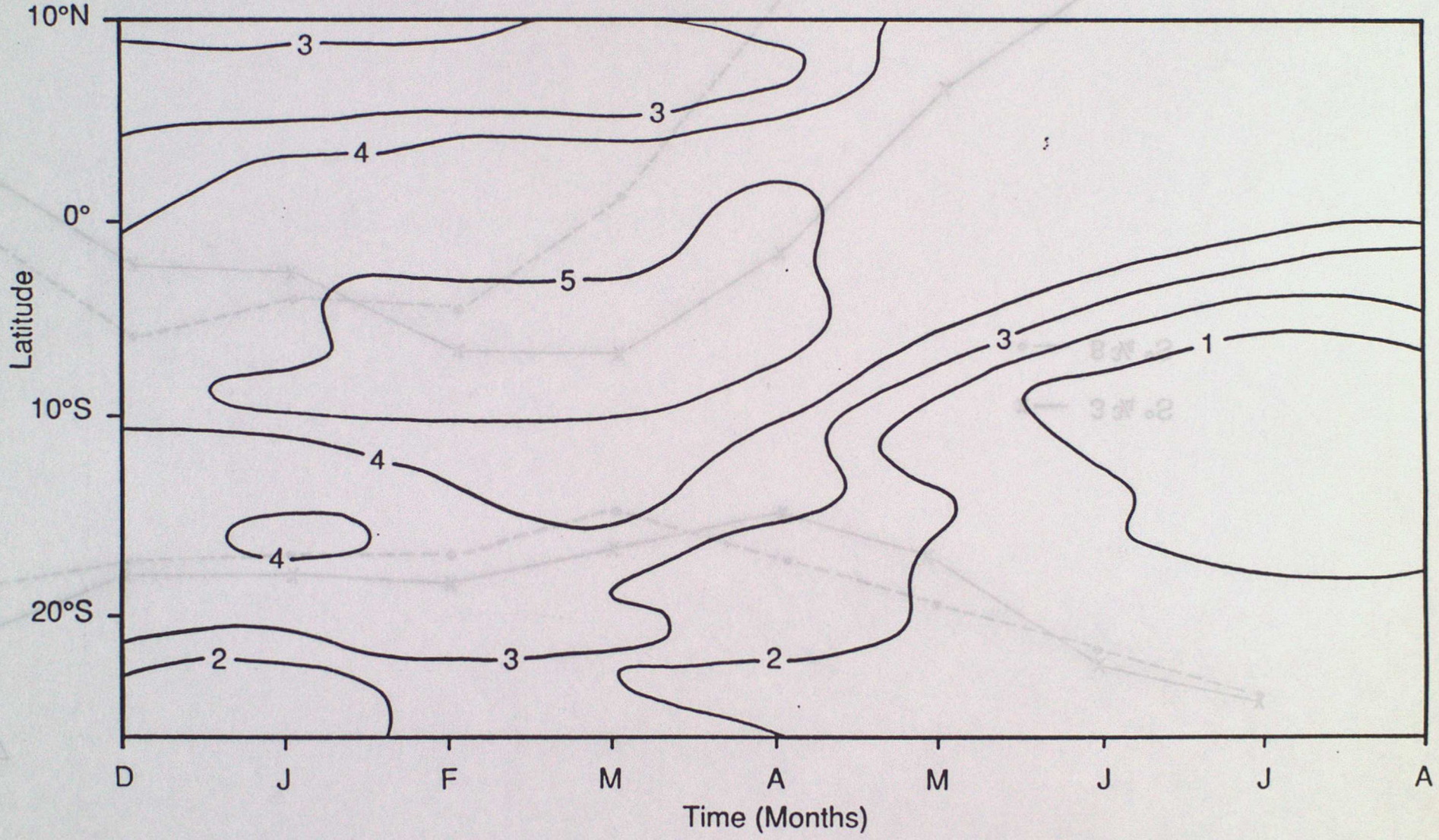

Figure 7

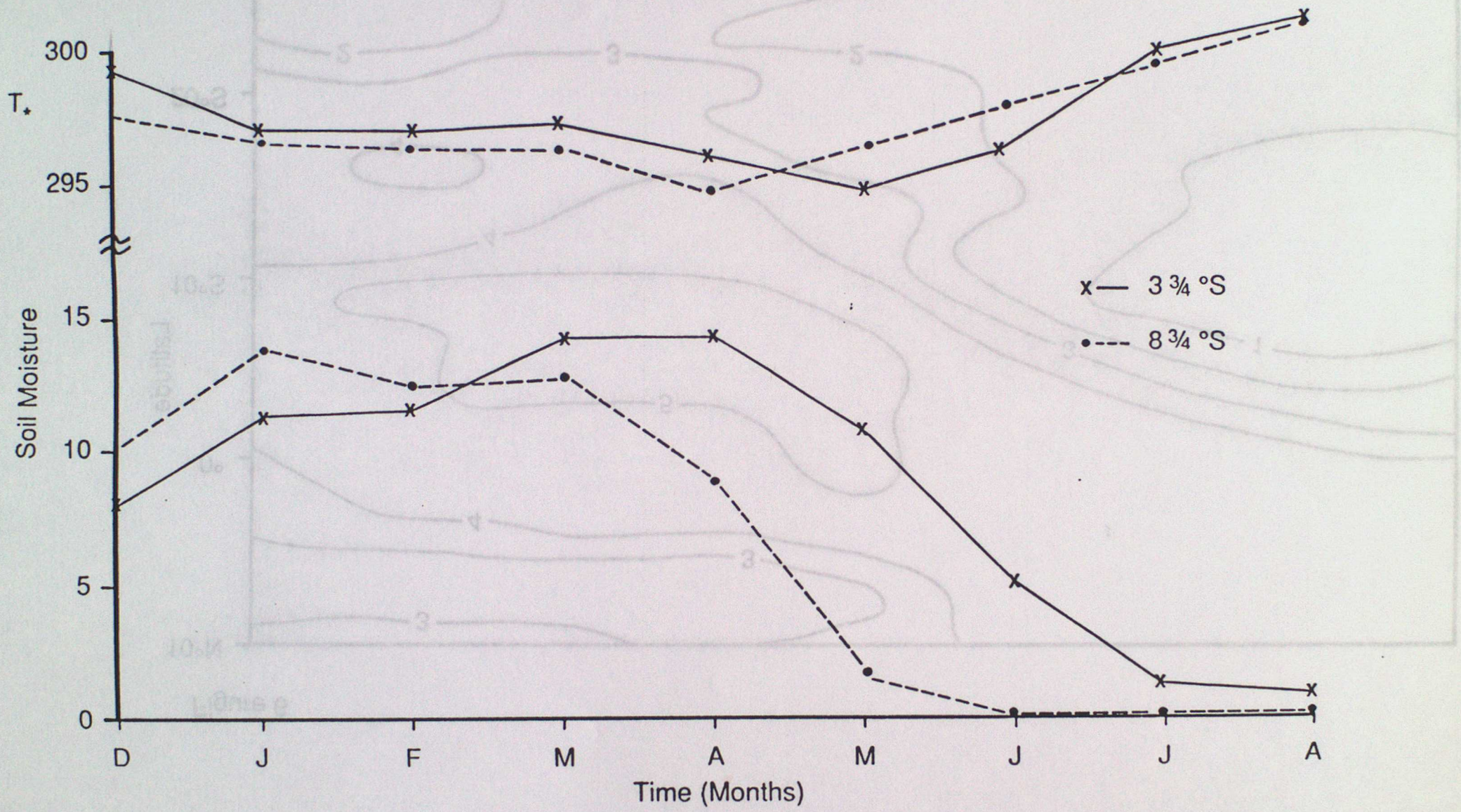
300
T*
295
Soil Moisture
15
10
5
0
D
J
F
M
A
M
J
J
A
Time (Months)
3 ¾ °S
8 ¾ °S

Figure 8a

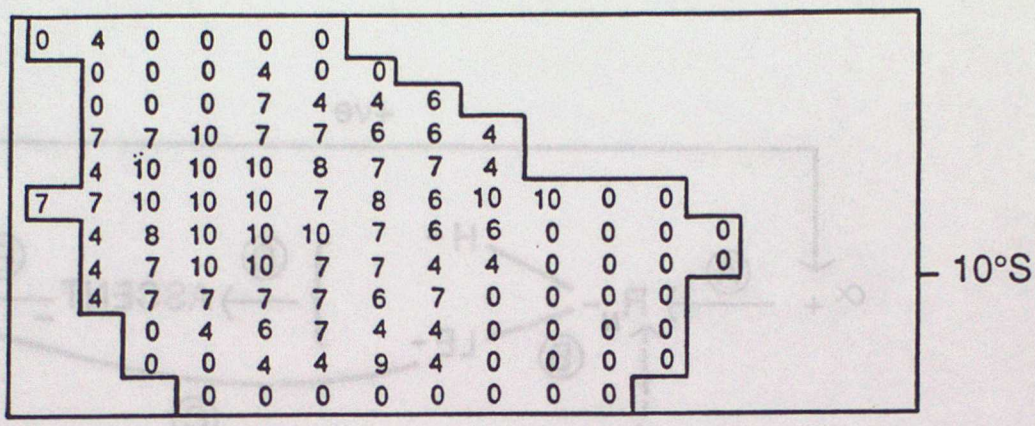

Figure 8b

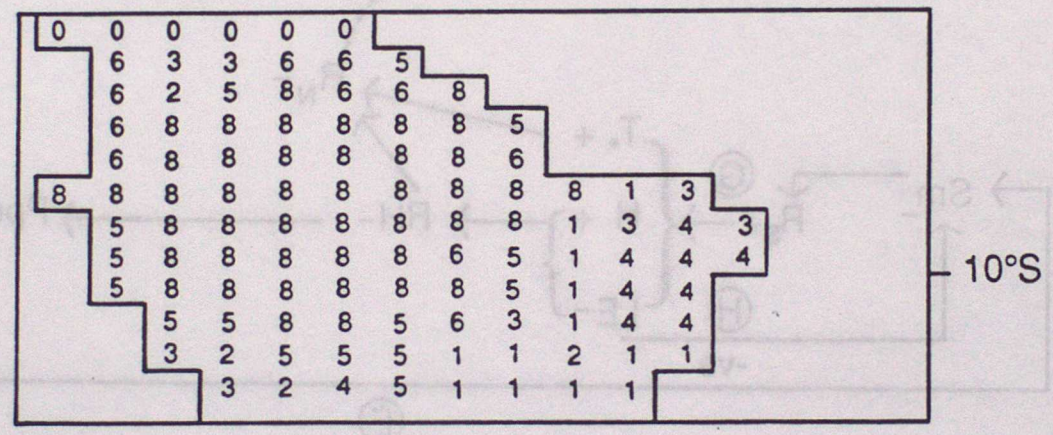

Figure 9

Some vegetation-Climate Interactions.

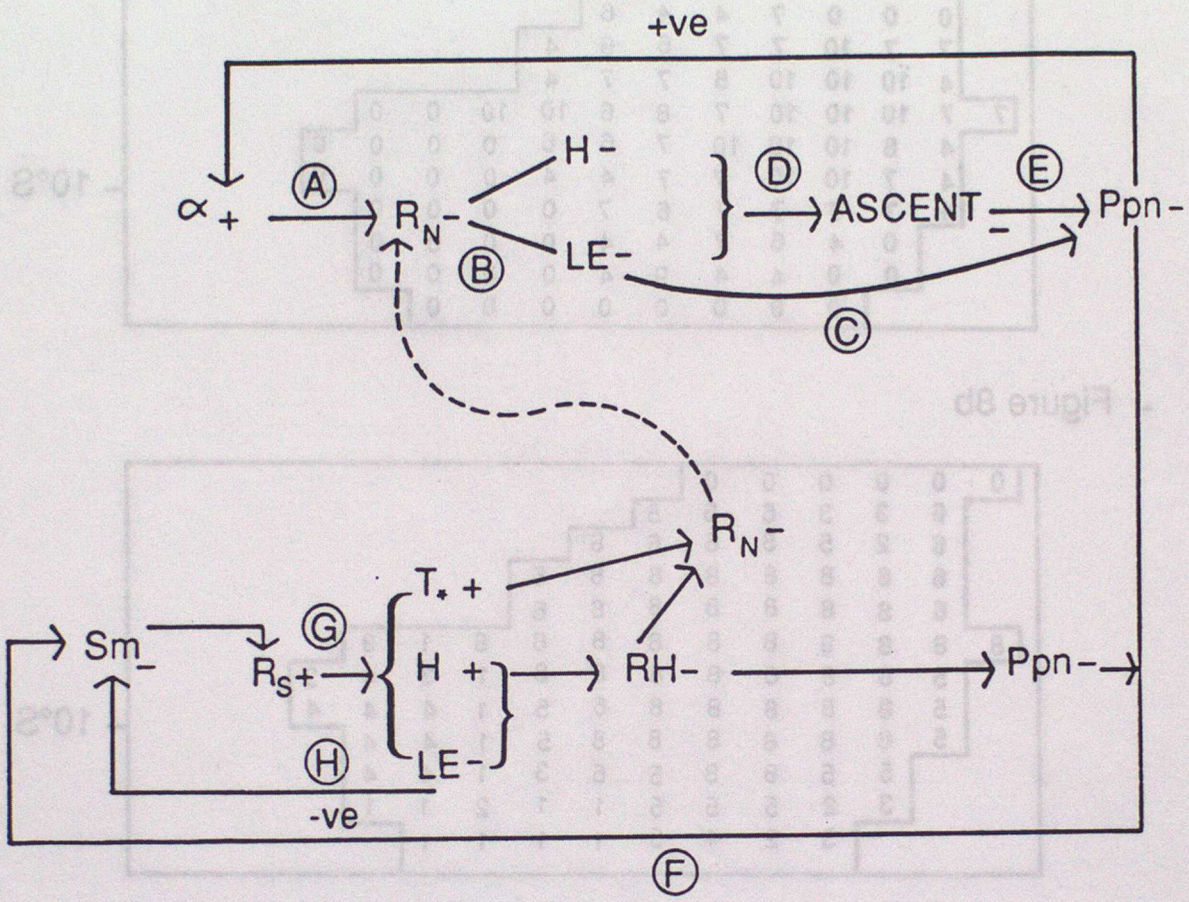

Ⓧ	process	LE	latent heat
α	albedo	Ppn	Precipitation
R_N	Net Radiation	RH	Relative humidity
H	Sensible heat	R_S	Surface resistance
Sm	Soil moisture	T_*	surface temperature

Figure 10a

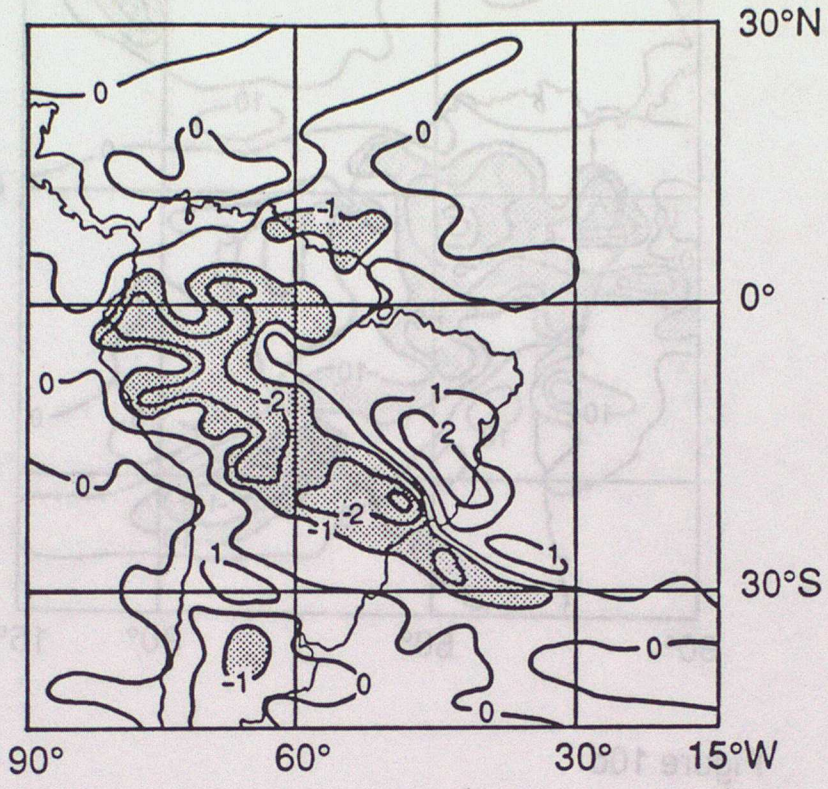

Figure 10b

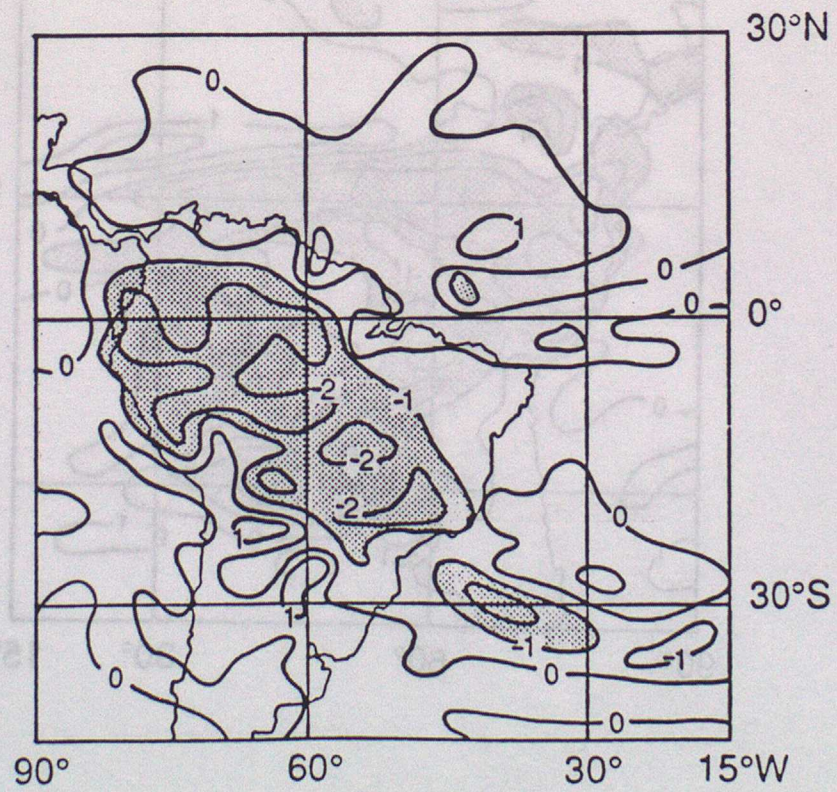

Figure10c

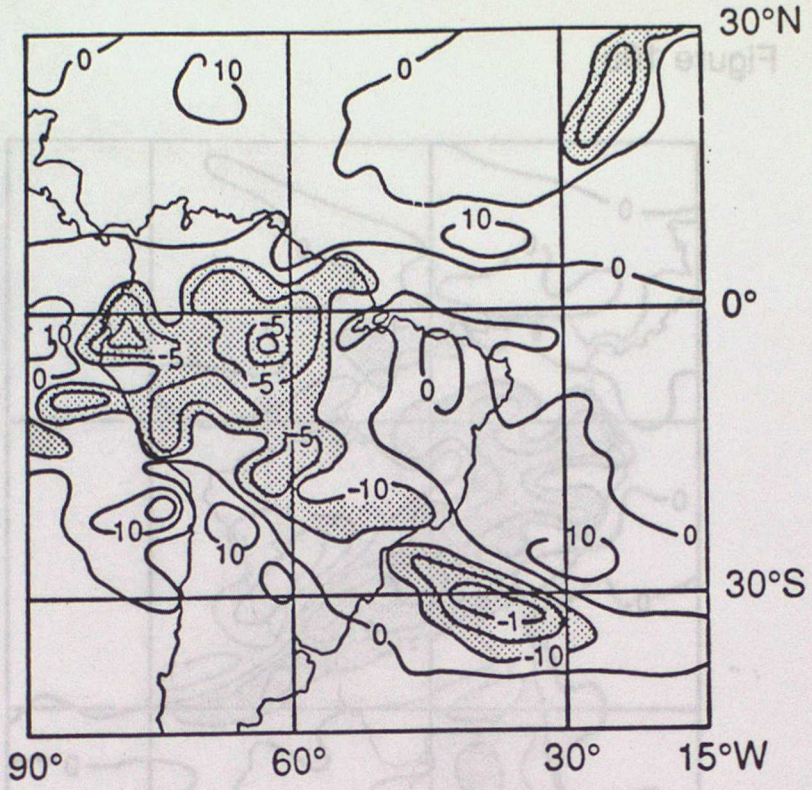

Figure 10d

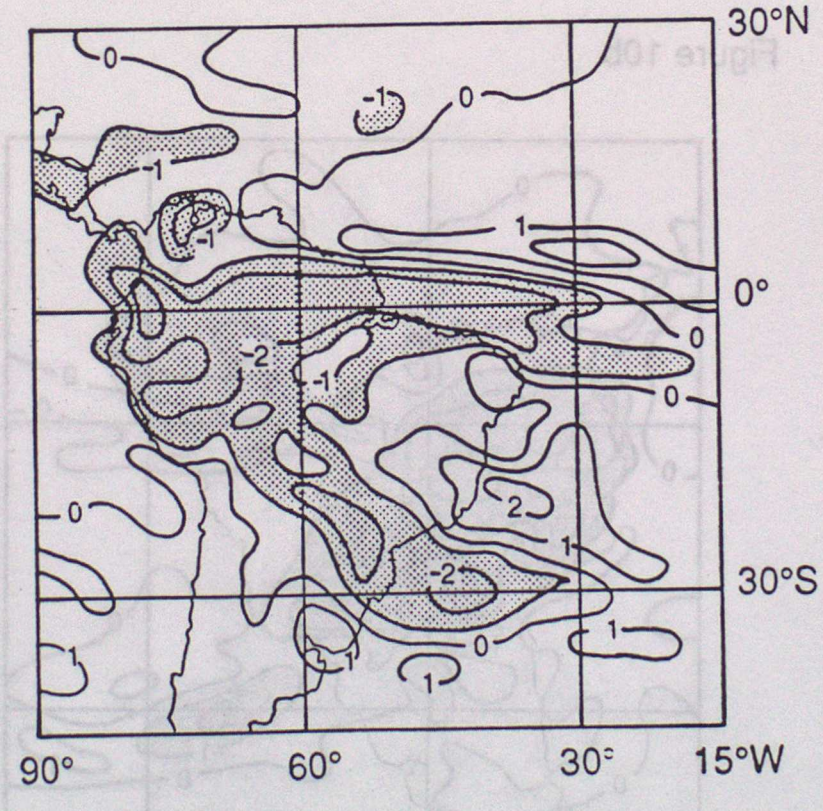

Figure 10e

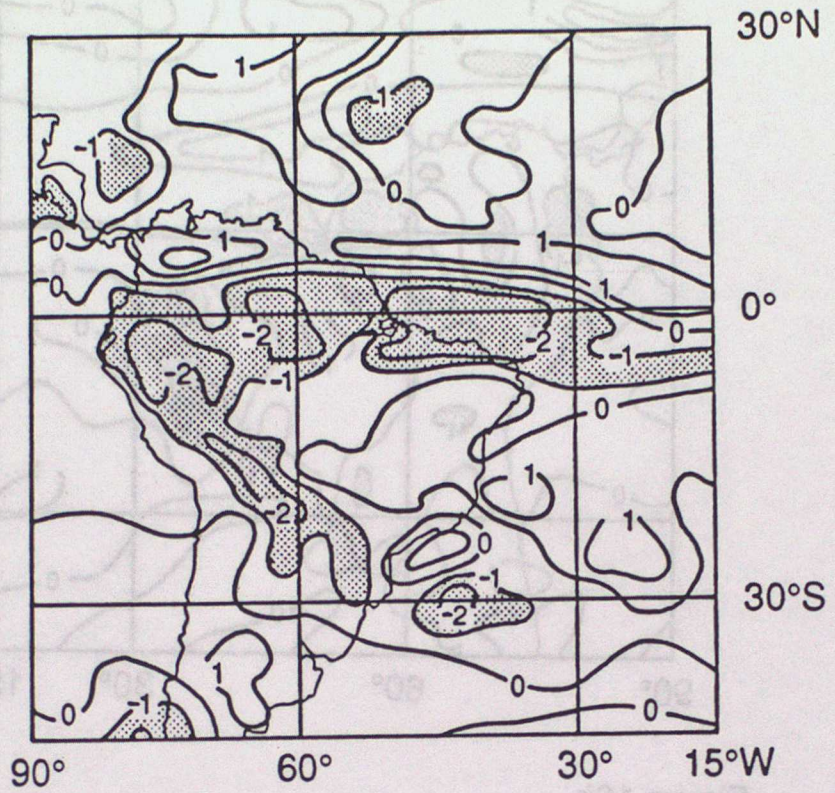

Figure 10f

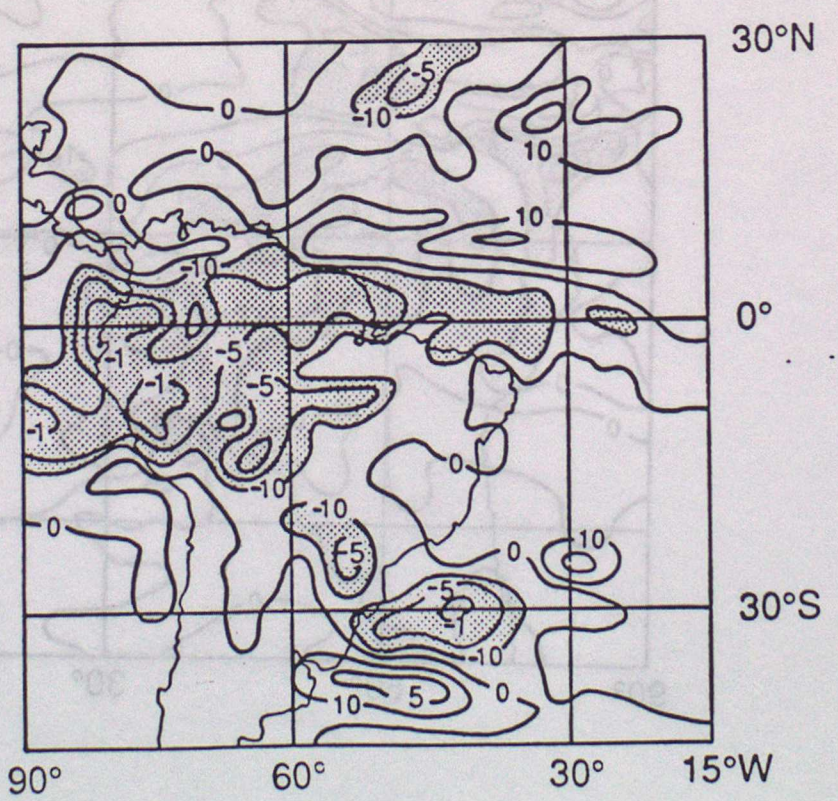

Figure 10g

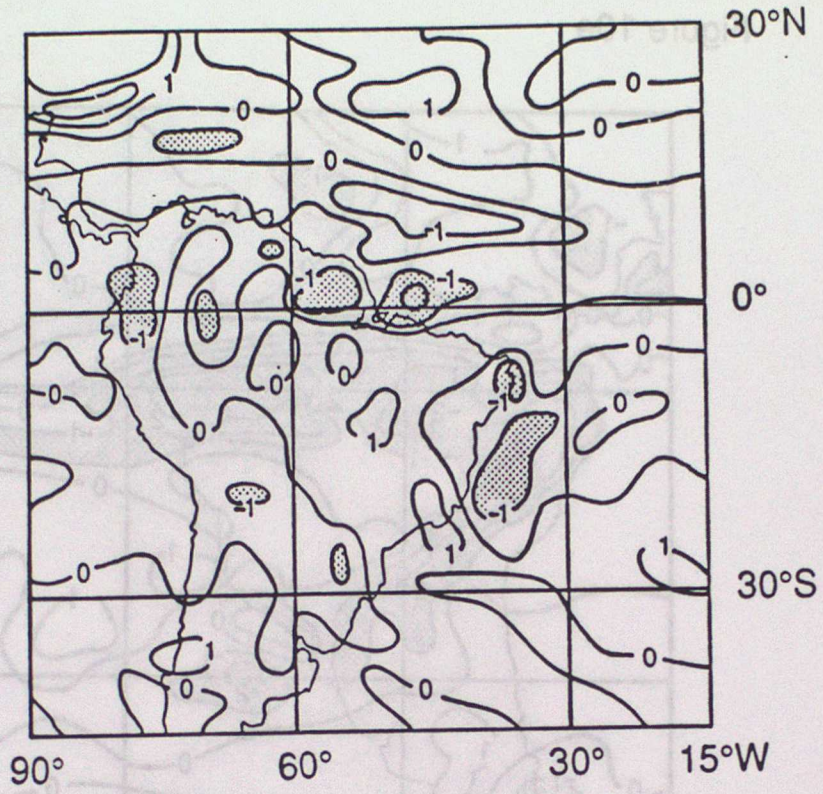

Figure 10h

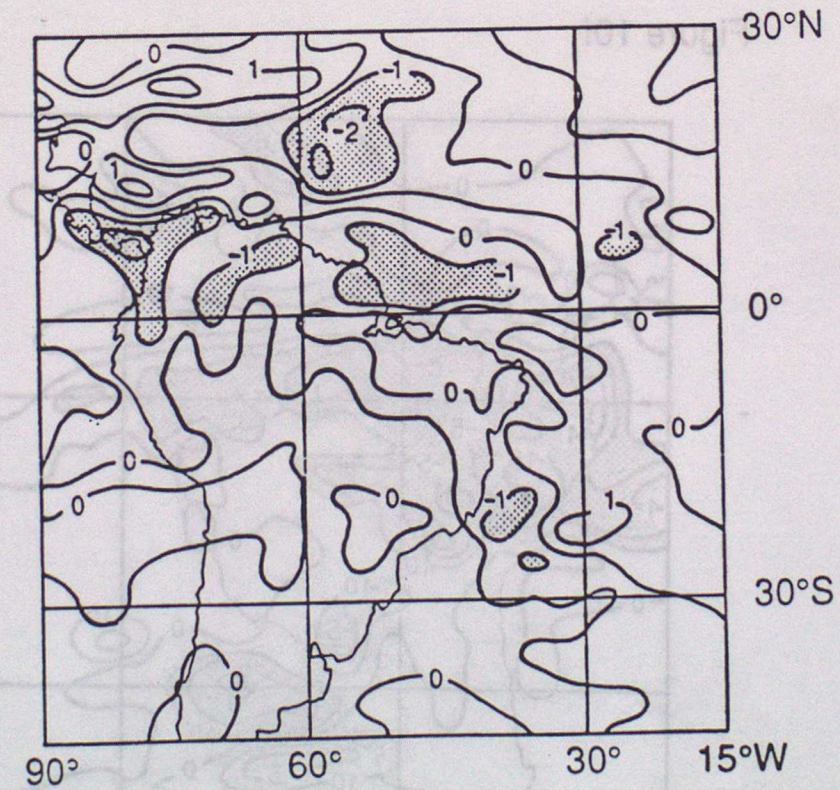

Figure 10i

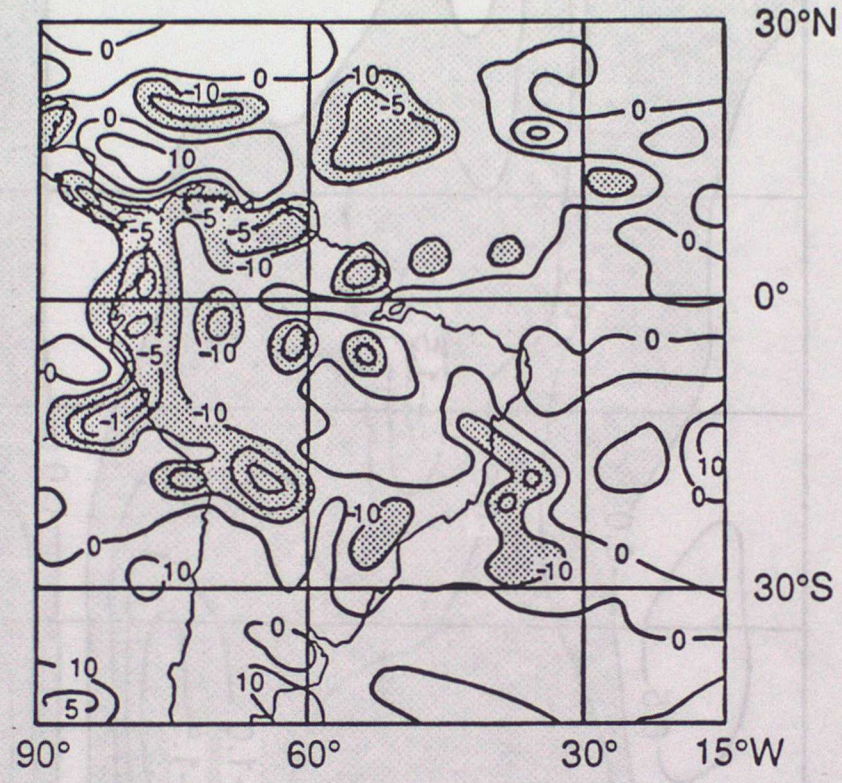

Figure 11

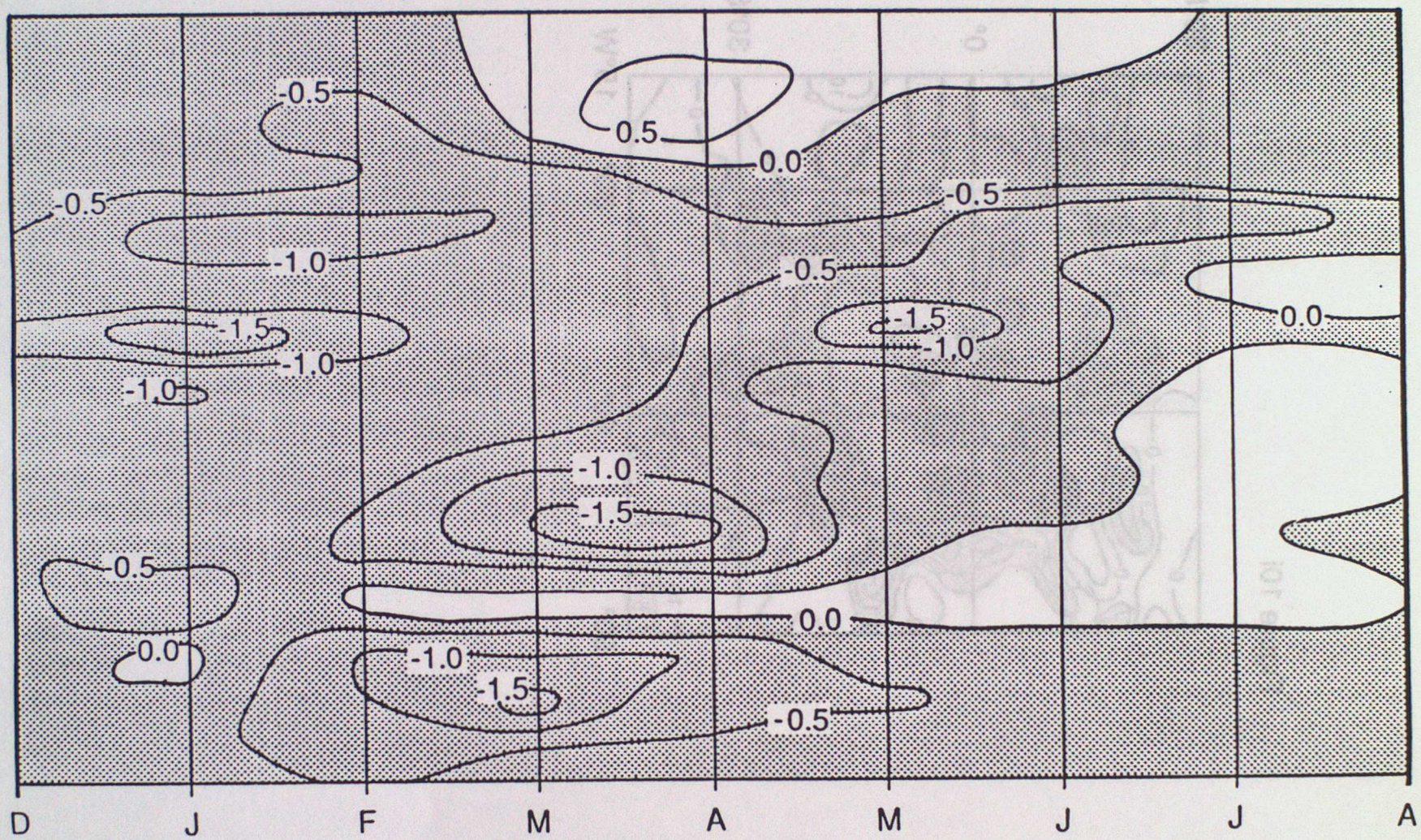
-0.5
0.5
0.0
-0.5
-0.5
-1.0
-0.5
-1.5
-1.0
0.0
-1.5
-1.0
-1.0
-1.0
-1.5
-0.5
0.0
0.0
-1.0
-1.5
-0.5
D
J
F
M
A
M
J
J
A

Figure 12

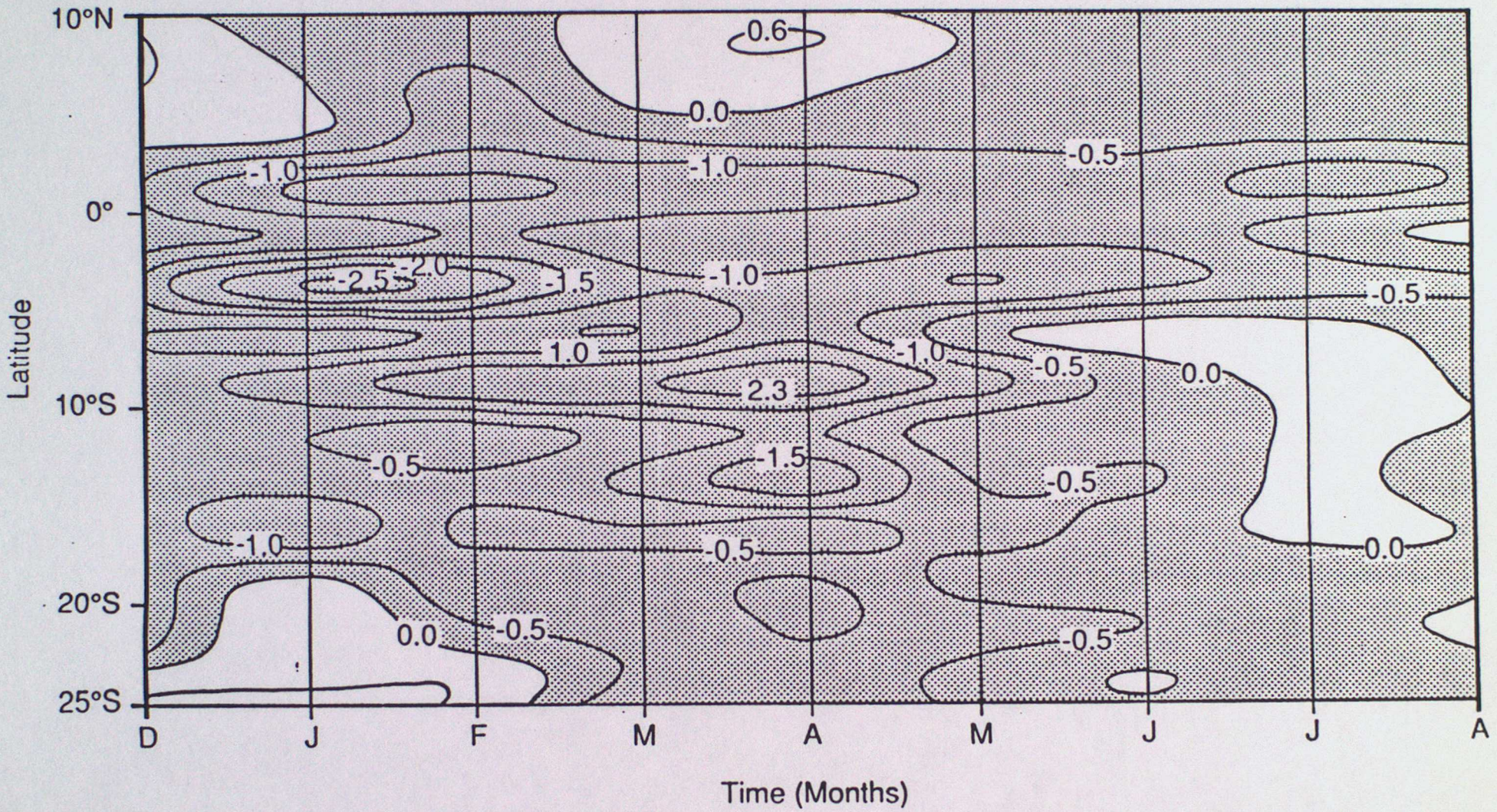
10°N
0°
10°S
20°S
25°S
Latitude
D
J
F
M
A
M
J
J
A
Time (Months)
0.6
0.0
-0.5
-1.0
-1.0
-2.0
-2.5
-1.5
-1.0
-0.5
1.0
-1.0
-0.5
0.0
2.3
-0.5
-1.5
-0.5
-1.0
-0.5
0.0
0.0
-0.5
-0.5

CLIMATE RESEARCH TECHNICAL NOTES

CRTN 1	Oct 1990	Estimates of the sensitivity of climate to vegetation changes using the Penman-Monteith equation. P R Rowntree
CRTN 2	Oct 1990	An ocean general circulation model of the Indian Ocean for hindcasting studies. D J Carrington
CRTN 3	Oct 1990	Simulation of the tropical diurnal cycle in a climate model. D P Rowell
CRTN 4	Oct 1990	Low frequency variability of the oceans. C K Folland, A Colman, D E Parker and A Bevan
CRTN 5	Dec 1990	A comparison of 11-level General Circulation Model Simulations with observations in the East Sahel. K Maskell
CRTN 6	Dec 1990	Climate Change Prediction. J F B Mitchell and Qing-cun Zeng
CRTN 7	Jan 1991	Deforestation of Amazonia - modelling the effects of albedo change. M F Mylne and P R Rowntree